Current transport through low-angle grain boundaries in high-temperature superconductors

A. Gurevich
Applied Superconductivity Center, University of Wisconsin, Madison, Wisconsin 53706

E. A. Pashitskii
Institute of Physics, National Academy of Sciences of Ukraine, Kiev, 252650, Ukraine

(Received 4 November 1997)

We consider mechanisms which can account for the observed rapid decrease of the critical current density $J_c(\theta)$ with the misorientation angle θ through grain boundaries (GB's) in high-T_c superconductors (HTS's). We show that the $J_c(\theta)$ dependence is mostly determined by the decrease of the current-carrying cross section by insulating dislocation cores and by progressive local suppression of the superconducting order parameter ψ near GB's as θ increases. The insulating regions near the dislocation cores result from a strain-induced local transition to the insulating antiferromagnetic phase of HTS's. The structure of the nonsuperconducting core regions and current channels in GB's is strongly affected by the anisotropy of the strain dependence of T_c which is essentially different for $YBa_2Cu_3O_7$ and Bi-based HTS's. We propose a mechanism of the progressive superconductivity suppression on GB's with θ due to an excess ion charge on the GB's which shifts the chemical potential in the layer of the order of screening length l_D near the GB's. The local suppression of ψ is amplified by the proximity of all HTS's to a metal-insulator transition, by their low carrier density and extended saddle point singularities in the electron density of states near the Fermi surface. Taking into account these mechanisms, we calculated $J_c(\theta)$ analytically by solving the Ginzburg-Landau equation. The model well describes the observed quasiexponential decrease of $J_c(\theta)$ with θ for many HTS's. The d-wave symmetry of the order parameter weakly affects $J_c(\theta)$ in the region of small θ and cannot account for the observed drop of $J_c(\theta)$ by several orders of magnitude as θ increases from 0 to $\theta \simeq 20°-40°$. [S0163-1829(98)06121-9]

I. INTRODUCTION

Mechanisms of current transport through grain boundaries (GB's) in high-temperature superconductors (HTS's) have attracted much attention. The critical current density $J_c(\theta)$ through GB's is very sensitive to the orientation of the adjacent crystallites and strongly decreases with the misorientation angle θ in the range from $\theta \simeq 3°-5°$ to $\theta \simeq 30°-40°$.[1–7] The d-wave symmetry of the order parameter in HTS's also contributes to the decrease of $J_c(\theta)$ with θ and gives rise to novel effects, such as π junctions and fractional vortices on GB's.[8–12] The rapid decrease of $J_c(\theta)$ with θ essentially limits the current-carrying capability of HTS materials which inevitably contain GB networks or colonies of misoriented grains.[13–18] For instance, the decrease of the fraction of high-angle GB's in biaxially textured HTS's substantially increased the critical current to a higher level determined by vortex dynamics and pinning, rather than by the GB transparency.[19–21]

A conventional model[22,23] describes a symmetric low-angle GB's as a chain of edge dislocations with the Burgers vector **b** perpendicular to the GB plane (Fig. 1). The structure of GB's in HTS's can be more complicated than the idealized one shown in Fig. 1 due to partial GB dislocations, faceting, long-range strain fields, and compositional variations near GB's.[24–31] These factors give rise to structural and chemical inhomogeneities along GB's on a broad variety of scales, from the nanoscale of individual dislocation cores to the macroscale of GB facets. Yet even in those rare cases when the atomic structure of a GB is known, the effect of this structure on superconducting properties remains unclear, since the correlation between atomic displacements and a microscopic mechanism of high-T_c superconductivity is still uncertain. In general, the material inhomogeneities along GB's cause modulations of the superconducting coupling across GB's which determines its global critical current density J_c after averaging the microscopic supercurrents $j(x)$ over the relevant spatial scales.

The GB dislocation structure naturally accounts for the decrease of $J_c(\theta)$, if one assumes that there are regions of a suppressed superconducting order parameter Δ near the dislocation cores which block the supercurrent through GB's.[1] These nonsuperconducting core (NC) regions of radius $r_i \sim b$ can result from local compositional and hole concentration variations, additional electron scattering, and significant

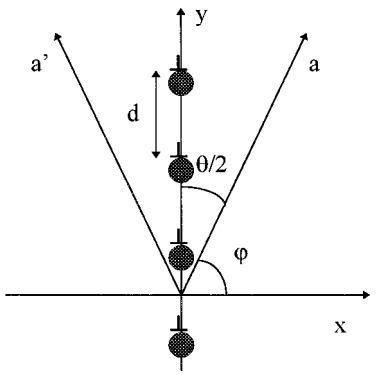

FIG. 1. Chain of edge dislocations which form a symmetric low-angle grain boundary in the y-z plane. The nonsuperconducting core regions are shadowed.

strains near the dislocation cores. High-resolution electron microscopy has shown that the low-angle GB's do consist of chains of edge dislocations separated by regions of a weakly distorted crystalline lattice and also exhibit compositional variations and strain fields near the Cu-rich dislocation cores on the scale $\simeq 10-300$ Å both along and across GB's.[24–31]

The dislocation model predicts the critical misorientation angle $\theta_c = 2\sin^{-1}(b/4r_i) \simeq 20°-40°$, above which the NC regions overlap, and GB's become a continuous insulating or normal Josephson contact with J_c much smaller than the intragrain critical current density J_g. For $\theta < \theta_c$, this model gives an approximately linear dependence $J_c(\theta) \simeq (1 - \theta/\theta_c)J_g$, if one assumes that $J_c(\theta)$ is determined by the area of current channels in GB's between the dislocation cores.[4] However this linear dependence $J_c(\theta)$ is much weaker than $J_c(\theta) \propto \exp(-\theta/\theta_0)$ with $\theta_0 \simeq 4°-5°$, which is usually observed experimentally.[1–7] Models have been proposed in which the current channels in GB's are described as an array of parallel point contacts[32–34] which exhibit weak-link behavior, if their width becomes smaller than the superconducting coherence length ξ,[35] that is, $d - 2r_i < \xi$, or $\theta < \theta_1 \simeq b/[\xi(T) + 2r_i]$. At 77 K, the in-plane $\xi(T)$ is about 35 Å, whence $\theta_1 \approx 5°$ for $r_i = b = 3.8$ Å, which correlates with the observed sharp decrease of $J_c(\theta)$ above $\theta \simeq 3°-7°$.[1,7]

The theoretical description of the observed dependence $J_c(\theta)$ remains incomplete, not least because of a variety of relevant physical mechanisms and the multiscale heterogeneity of GB's. The rapid decrease of $J_c(\theta)$ is usually ascribed to the strain-induced, or compositional suppression of Δ near dislocation cores and in the layer of thickness $l(\theta)$ near GB's.[24–41] Then the array of parallel current channels in GB's is regarded as an effective Josephson contact, for which

$$J_c \propto \exp[-l(\theta)/\xi_N(\theta)], \quad l \gg \xi_N, \tag{1}$$

where ξ_N is the characteristic decay length which can be the proximity length for metallic GB's or the tunneling length for insulating GB's.[5] Thus, basically any increase of $l(\theta)$ with the dislocation density $b/d \simeq \theta$ or decrease of ξ_N due to additional electron scattering on GB's dislocations and compositional variations near GB's could account for the observed rapid decrease of $J_c(\theta)$ with θ. However, this phenomenological approach has several inconsistencies. First, Eq. (1) can be used for a clean metallic GB, provided that $l > 2\xi_N \simeq 2\xi(0)T_c/T$. This implies a fairly wide layer of suppressed order parameter near the GB ($l > 600$ Å at 4.2 K), which would result in negligible J_c at 77 K. Yet, the weak-link behavior of GB's and strong decrease of $J_c(\theta)$ have been observed both at 4.2 and 77 K, with J_c at 77 K exhibiting rather high values $\sim 10^5$ A/cm^2 in thin film $YBa_2Cu_3O_7$ bicrystals.[3,5–7] Second, the strain fields of a symmetric GB exponentially decay over the length $l = d/2\pi$,[22] which *decreases* as θ increases. To account for the increase of $l(\theta)$ with θ, one has to assume nonperiodicity of the GB dislocation structure and distribution of d,[41] compositional variations near GB's, macroscopic strain fields produced by the GB facets,[31] etc. The periodic long-range strains near low-angle GB's can even locally *increase* T_c for small θ and depress T_c at larger θ due to proximity effect coupling of the NC core regions.[42] For the d-wave symmetry of the order parameter, faceting can also cause decreasing $J_c(\theta)$,[10] but this mechanism gives the relatively weak dependence $J_c \propto \cos^2 2\theta$ which is not sufficient to explain the observed drop in $J_c(\theta)$ by two to three orders of magnitude without the assumption of the local depression of Δ on the GB's. The gap suppression due to local nonstoichiometry near the GB's is mostly determined by materials factors, such as diffusion of oxygen in remanent strain fields around GB's which may contribute to the significant scatter in $J_c(\theta)$ usually observed on HTS bicrystals of the same misorientation θ.[5,7] However, the nearly ''universal'' dependence $J_c(\theta) \propto \exp(-\theta/\theta_0)$ observed on many HTS's (Refs. 5 and 6) seems to indicate a fundamental intrinsic mechanism of the GB weak-link behavior common for all HTS's.

In this paper we propose a model which describes the observed $J_c(\theta)$, taking into account the GB dislocation structure and the fact that a comparatively small shift of the chemical potential μ near GB's can strongly decrease T_c, or even turn HTS's into an insulating antiferromagnet.[50] Because of the proximity of HTS's to the metal-insulator transition, the strains and excess ion charge of the GB dislocation structure can locally induce a dielectric phase near dislocation cores and cause progressive overall suppression of the superconducting order parameter with θ in a narrow layer of the order of the screening length near GB's. The model provides an intrinsic mechanism for the rapid decrease of $J_c(\theta)$ with θ and describes well the observed $J_c(\theta)$ dependence in HTS bicrystals, even without invoking the local nonstoichiomentry and heterogeneity of GB's. For small θ, the local suppression of superconductivity at GB's is shown to affect $J_c(\theta)$ much more strongly than the symmetry of the order parameter which manifests itself at higher θ. We obtain $J_c(\theta)$ by solving the Ginzburg-Landau (GL) equation which describes well the practically important temperature range $T > 77$ K for HTS's.

The paper is organized as follows. In Sec. II we discuss mechanisms which determine the structure of the NC regions and the gap suppression near GB's. We first consider a strain mechanism which gives rise to a composite structure of the NC regions consisting of a dielectric core surrounded by a normal shell. The shape of the NC regions is strongly affected by the in-plane anisotropy of the strain dependence of T_c. Then we consider the electron screening of the excess ion charge of GB's which results in superconducting gap suppression near the GB's amplified by the proximity of HTS's to the metal-insulator transition, low carrier density, and extended saddle point singularities near the Fermi surface. In Sec. III we propose a model described by the GL equation which takes into account the current channel structure of a low-angle GB's and the local gap suppression near GB's. This exactly solvable nonlinear model enabled us to obtain an analytical formula for $J_c(\theta)$ which gives a strong (though nonexponential) decrease of $J_c(\theta)$ with θ. In Sec. IV we compare the model with experiment and show that the theoretical $J_c(\theta)$ dependence describes well the observed $J_c(\theta)$ in $YBa_2Cu_3O_7$ and Bi-based HTS's.

II. CURRENT CHANNELS IN GB's

A. Strain mechanism

A qualitative description of NC regions can be made, assuming that the superconducting coupling constant $\lambda(\mathbf{r})$ near

the dislocation core becomes spatially inhomogeneous due to its dependence on the local strain tensor ϵ_{ik}. The suppression of Δ near the cores can be quantified in terms of the tensor C_{ik} which determines the shift of T_c in a weakly deformed superconductor:

$$T_c = T_{c0} - C_{ik}\epsilon_{ik}. \tag{2}$$

The strain dependence of T_c in HTS's can be highly anisotropic.[43–47] For instance, for optimally doped $YBa_2Cu_3O_7$ single crystals, it was found that $dT_c/dp_a = -(1.9–2)$ K/GPa, $dT_c/dp_b = 1.9–2.2$ K/GPa, and $dT_c/dp_c = -(0–0.3)$ K/GPa,[45] where p_i is the stress along the ith axes. The hydrostatic pressure derivative $dT_c/dp = \Sigma_i dT_c/dp_i$ yields a comparatively small value $dT_c/dp \simeq 0.3$ K/GPa which results from a cancellation of large, almost equal, and opposite in-plane effects of different signs. This is usually ascribed to the influence of Cu-O chains, orthorhombic distortions of the Cu-O planes, charge transfer effects, etc.[43–46] By contrast, $Bi_2Sr_2CaCu_2O_x$ exhibits nearly isotropic in-plane pressure derivatives $dT_c/dp_a \simeq 1.6$ K/GPa, $dT_c/dp_b \simeq 2$ K/GPa, but large negative $dT_c/dp_c \simeq -2.8$ K/GPa along the c axis, so that $dT_c/dp = \Sigma_i dT_c/dp_i$ again largely cancels under hydrostatic pressure. Doping can substantially affect dT_c/dp_i; for example, the dT_c/dp_i values for underdoped $YBa_2Cu_3O_7$ with $T_c \approx 40$ K are about 2–10 times larger than those for the optimally doped $YBa_2Cu_3O_7$.[48]

For planar deformations, Eq. (2) becomes

$$\delta T_c = -C[\epsilon + p(\epsilon_{xx} - \epsilon_{yy})\cos 2\varphi + 2p\epsilon_{xy}\mathrm{sgn}(x)\sin 2\varphi], \tag{3}$$

where $p = (C_a - C_b)/(C_a + C_b)$, $\epsilon = \epsilon_{xx} + \epsilon_{yy}$, $C = (C_a + C_b)/2$, and φ is the angle between the x axis taken along the normal to the GB's and the a axis in Fig. 1. The constants $C_a = -\partial T_c/\partial\epsilon_{aa}$ and $C_b = -\partial T_c/\partial\epsilon_{bb}$ determine the change of T_c under uniaxial compression ($\epsilon_i < 0$); for example, $C_a = -217$ K and $C_b = 316$ K for optimally doped $YBa_2Cu_3O_{7-\delta}$ single crystals.[47] For $C_a = C_b$, which corresponds to the nearly isotropic in-plane dependence $T_c(\epsilon_{ik})$ found in $Bi_2Sr_2CaCu_2O_x$ (Bi-2212), Eq. (3) reduces to $\delta T_c = -C\epsilon$. Assuming isotropic elastic constants in the ab plane,[49] the shape of the NC region for a single edge dislocation can be evaluated from the condition $T_c(\mathbf{r}) = 0$, using Eq. (3) with $\varphi = 0$ and ϵ_{ik} from Appendix A. For the dislocation at $x = y = 0$, the boundary of the NC region is described by

$$r(\phi) = 2r_0 \sin\phi(1 + p_0\cos^2\phi), \tag{4}$$

$$r_0 = \frac{bC(1-2\sigma)}{4\pi T_{c0}(1-\sigma)}, \quad p_0 = \frac{C_a - C_b}{(1-2\sigma)(C_a + C_b)}, \tag{5}$$

where σ is the Poisson ratio and ϕ is the polar angle. For the isotropic strain dependence of T_c, Eq. (4) describes a circle of radius r_0 centered at $x = 0, y = -r_0$ [Fig. 2(a)]. For anisotropic $T_c(\epsilon_{ik})$ with $|p_0| \gg 1$, the characteristic size of the NC region becomes $r_1 = r_0|p_0|$, and its shape changes as shown in Figs. 2(b) and 2(c).

Figure 2 shows the NC regions in a grain boundary calculated from the condition $T_c(\mathbf{r}) = 0$, where T_c is given by Eq. (3), $2\varphi = \pi - \theta$, and ϵ_{ik} for the periodic chain of GB dislocations is taken from Appendix A. For isotropic $T_c(\epsilon_{ik})$,

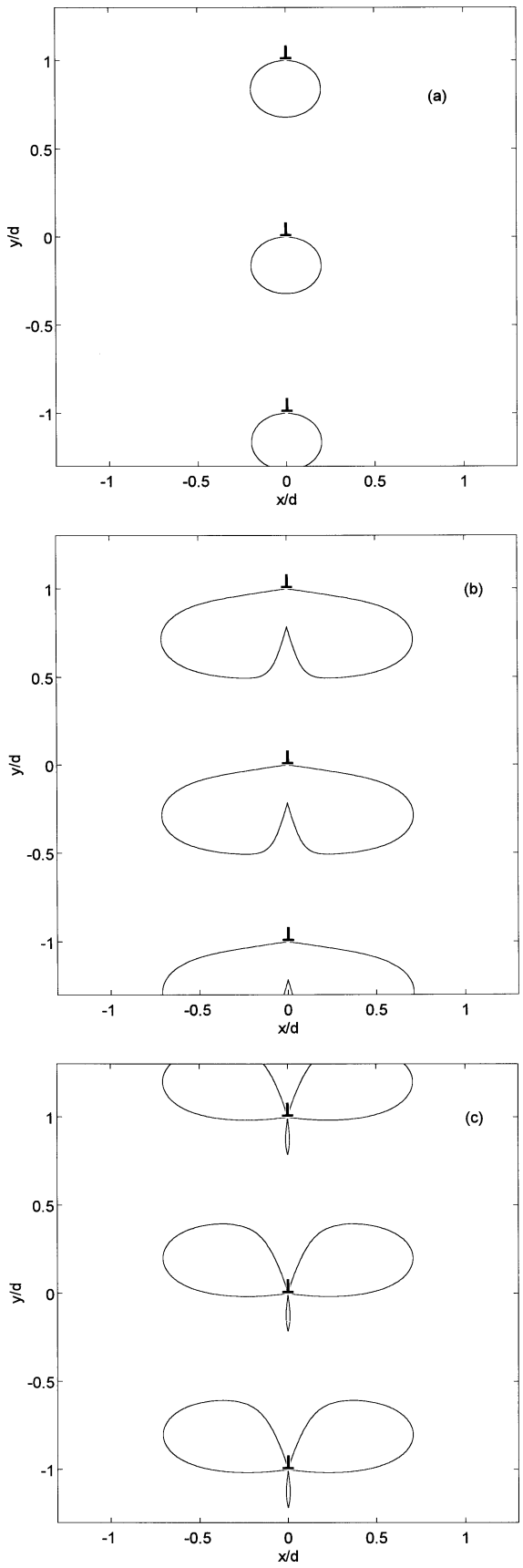

FIG. 2. Nonsuperconducting core regions in a symmetric GB calculated from Eq. (3) for $\theta = 15°$ and $\sigma = 0.28$. (a) shows the isotropic case $p = 0$ for $C/T_{c0} = 20$. (b) and (c) show the NC regions for the anisotropic case: $C/T_{c0} = 10$, $p = 5.3$ (b) and $C/T_{c0} = 10$, $p = -5.3$ (c).

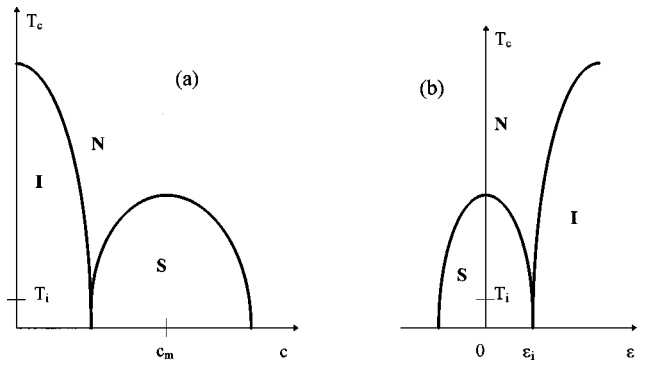

FIG. 3. Phase diagram $T(c)$ of high-T_c superconductors (a), where I, N, and S correspond to the insulating, normal, and superconducting states, respectively. (b) shows (a) replotted in the T-ϵ coordinates.

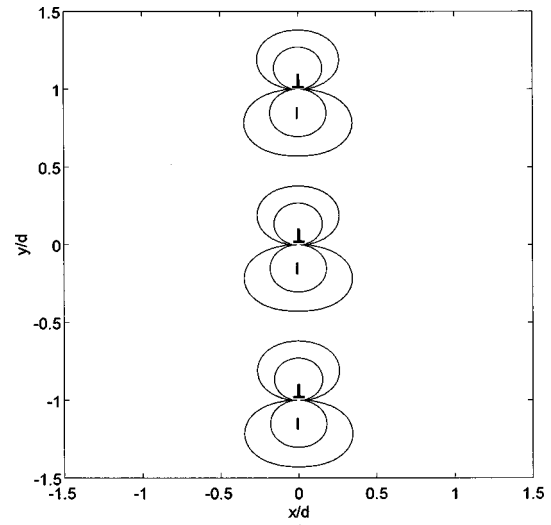

FIG. 4. Composite structure of the nonsuperconducting core regions in a GB for the isotropic case calculated from Eq. (7) for $\theta = 15°$, $T = 77$ K, $\Delta T_m = 1$ K, $C = 300$ K, $T_{c0} = 90$ K, and $\sigma = 0.28$. The inner region (I) is in an insulating state surrounded by the normal regions.

the NC regions shrink and flatten along GB's as θ increases, but they do not touch for any d. The latter is due to partial compensation of the dipole strain fields of GB dislocations, resulting in the exponential decay of $\epsilon_{ik} \propto \exp(-2\pi|x|/d)$ away from GB's. For anisotropic $T_c(\epsilon_{ik})$, the NC regions do not overlap as well, though their shape depends on the sign of p and can significantly differ from the isotropic case. As an illustration, Figs. 2(b) and 2(c) show NC regions for typical $YBa_2Cu_3O_{7-\delta}$ values $p = \pm 5.3$, where the plus sign corresponds to the case shown in Fig. 1, and the minus sign corresponds to the transposition of the a and b axes. For the anisotropic strain dependence of T_c, the current-carrying cross section of GB's can be strongly reduced by off-diagonal components of ϵ_{ik}. This may contribute to the weak-link behavior of [001] tilt GB's in the basal plane of $YBa_2Cu_3O_{7-\delta}$.

The above description, based on the linear strain dependence (2), can be used for NC regions much larger than b. This implies $C \gg T_{c0}$ in Eq. (5), which corresponds to underdoped HTS,[43–46] or significant local nonstoichiometry near GB's. However, for optimally doped HTS's ($\sigma = 0.28$, $C \simeq 300$ K, and $T_{c0} \simeq 100$ K), Eq. (4) yields a fairly small diameter of the NC region, $2r_0 \simeq 0.3b \simeq 1$ Å. This indicates that the linear approximation (2) of $T_c(\epsilon_{ik})$ is not self-consistent, since the elastic strains $\epsilon_{ij} \propto b/2\pi r_0$ near the dislocation cores become so strong that the linear expansion (3) of T_c in ϵ_{ij} is hardly adequate. Thus, we have to take account of the actual nonlinear dependence of T_c on ϵ_{ij} shown in Fig. 3 with a characteristic maximum at the optimum strain ϵ_m, which reflects the nonmonotonic dependence of T_c of HTS's on the hole concentration c on the Cu-O planes.[50,52] In the absence of structural transitions, $T_c(\epsilon)$ may be approximated by a conventional parabolic function, which describes well the observed dependence of T_c on hydrostatic pressure p in HTS's.[43–46] The general quadratic dependence $T_c(\epsilon_{ij})$ in anisotropic HTS's can be written in the form $T_c = T_{c0} - C_{ij}\epsilon_{ij} - Q_{ijkl}\epsilon_{ij}\epsilon_{kl}$, where the tensor Q_{ijkl} is symmetric with respect to the transposition $i \leftrightarrow j$ and $k \leftrightarrow l$, and the principal values C_a, C_b, and C_c of C_{ij} determine the observed $dT_c/d\epsilon_i$ for $\epsilon_{ij} \to 0$. For orthorhombic symmetry, Q_{ijkl} has nine independent components,[23] but for planar deformations Q_{ijkl} has four independent components; so

$$T_c = T_{c0} - C_a\epsilon_{aa} - C_b\epsilon_{bb} - Q_a\epsilon_{aa}^2 - Q_b\epsilon_{bb}^2 - Q_1\epsilon_{aa}\epsilon_{bb} - Q_2\epsilon_{ab}^2 . \quad (6)$$

The simplest version of Eq. (6) with $C_a = C_b$, $Q_a = Q_b = Q_1/2$, and $Q_2 = 0$ corresponds to a purely isotropic $T_c(\epsilon)$ which depends only on the dilatation ϵ,

$$T_c = T_{c0} - C\epsilon - (C\epsilon)^2/4\Delta T_m . \quad (7)$$

Here $\Delta T_m = T_{cm} - T_{c0}$, and the coefficients in Eq. (7) are chosen such that the maximum value of T_c equals T_{cm} at $\epsilon_m = -2\Delta T_m/C$, and $dT_c/d\epsilon$ gives the observed C at $\epsilon \to 0$. The pressure experiments have shown that $\Delta T_m \ll T_{c0}$, at least for optimally doped HTS's.[43–46] In this case $T_c(\epsilon)$ vanishes at comparatively weak strain $\epsilon_i \simeq \sqrt{2\Delta T_m T_{c0}}/C \ll 1$, for which the linear elasticity theory is still applicable, since $C > T_{c0}$.

Now we can estimate the size of the NC region for the nonlinear $T_c(\epsilon)$. For the isotropic $T_c(\epsilon)$, the condition $T_c = 0$ yields a quadratic equation for $\epsilon = b(1 - 2\sigma)\sin\phi/2\pi(1-\sigma)r$. Its solution gives two circular NC regions described by Eqs. (4) and (5) with $p_0 = 0$ and r_0 replaced by $r_i^{\pm}$ (Fig. 4). The radii $r_i^{\pm}$ are

$$r_i^{\pm} = \frac{r_0}{2}(\sqrt{1+\alpha_0} \pm 1), \quad (8)$$

where $\alpha_0 = T_{c0}/\Delta T_m$. For $\Delta T_m \ll T_c$, the nonlinearity of $T_c(\epsilon)$ increases r_i by the factor $(T_c/4\Delta T_m)^{1/2}$ as compared to r_0. For optimally doped Bi-2212, $\sigma = 0.28$, $C \simeq 300$ K, $T_{c0} \simeq 100$ K, and $\Delta T_m = 4$ K; we obtain from Eq. (8) that $2r_i^+ \approx b$. The local nonstoichiometry near the Cu-rich dislocation cores[24] may considerably increase the ratio C/T_{c0} in Eq. (8), thus further increasing r_i.

For the anisotropic $T_c(\epsilon_{ik})$ dependence (6), the solution of the quadratic equation $T_c[\epsilon_{ik}(r(\phi))] = 0$ for $r(\phi)$ yields

$$r(\phi)=r_0 \sin\phi[\sqrt{(1+2p_0\cos^2\phi)^2+g(\phi)} \pm(1+2p_0\cos^2\phi)], \quad (9)$$

$$g(\phi)=g_0+g_1(\cos^2\phi-\sigma\sin^2\phi) +g_2[(1-2\sigma)^2-4\cos^2\phi]+g_3 ctg^2\phi\cos^2\phi, \quad (10)$$

where $g_0=4QT_{c0}/C^2$, $g_1=4(Q_a-Q_b)T_{c0}/(1-2\sigma)C^2$, $g_2=(Q_1-2Q)T_{c0}/4(1-2\sigma)^2C^2$, $g_3=Q_2T_{c0}/4(1-2\sigma)^2C^2$, and $Q=(Q_a+Q_b)/2$. For the isotropic case, $\beta_0=g_1=g_2=g_3=0$, $Q=C^2/4\Delta T_m$, Eq. (9) reduces to Eq. (8). Unlike the isotropic case, the shape of $r(\phi)$ for the anisotropic case can be changed by the nonlinear terms in Eq. (6). We do not discuss here the anisotropic case in more detail because of a lack of experimental data on Q_i for $YBa_2Cu_3O_7$.

The structure of the NC regions may be further clarified by the phase diagram of HTS's $T_c(c)$, shown in Fig. 3. Indeed, using the electroneutrality condition, the isotropic strain dependence of $T_c(\epsilon)$ can be qualitatively mapped onto the domelike dependence of $T_c(c)$ on the hole concentration c, if $\epsilon(\mathbf{r})$ varies weakly on microscopic scales, such as the screening length (see below) and ξ. Figure 3 clearly shows that the slope $C=dT_c/d\epsilon$ increases as T_c decreases, giving the observed strong sensitivity of the ratio C/T_{c0} to the local doping level.[43–46,51] Under these assumptions, we can replot the phase diagram in T-ϵ coordinates as shown in Fig. 3(b) and conclude that for $T=0$ the NC regions are partly in an insulating (I) state,[5,24] since the point $T_c=0$ is close to the region of the HTS phase diagram which corresponds to an insulating antiferromagnet. Recent measurements of resistivity $\rho(T)$ of $La_{2-x}Sr_xCuO_4$ in high pulsed magnetic fields[52] revealed an insulating behavior of $\rho(T)$ even in the superconducting region of the phase diagram after suppression of the order parameter by a magnetic field. Therefore, the strains might cause the local S-I transition near the dislocation cores in larger domains determined by $T_c(\epsilon)=T_i$, where T_i corresponds to the intersection of the superconducting and insulating regions on the phase diagram in Fig. 3. The nonzero T_i can be taken into account by replacing T_{c0} with $T_{c0}-T_i$ in Eq. (8). Notice that Winkler *et al.*[53] reported on a significant dielectric fraction in GB's for a 32°[001] tilt $YBa_2Cu_3O_7$ bicrystal which manifests itself in Fiske resonances on I-V characteristics. A large T_c depression was also observed on a 7° Bi-2212 tilt bicrystals.[54]

The NC regions therefore have a composite structure consisting of insulating and normal domains, whose boundaries are defined by the conditions $T_c(\epsilon)\simeq T_i$ and $T_c(\epsilon)\simeq T$, as shown in Fig. 4. For a single dislocation, the dielectric domain is a circle of radius r_i^+ centered at $x=0$, $y=-r_i^+$ (as seen from Fig. 3, the second solution r_i^- for underdoped HTS's corresponds to a normal domain). The outer shape of the normal domain is two circles which touch at $x=y=0$, their radii $r_n^\pm$ being described by Eqs. (4) and (8) in which T_{c0} should be replaced by $T_{c0}-T$:

$$r_n^\pm=\frac{r_0}{2\tau}(\sqrt{1+\alpha_0\tau}\pm 1), \quad (11)$$

where $\tau=(T_{c0}-T)/T_{c0}$. The size of the normal NC region along GB's, $L_n=2(r_n^+ + r_n^-)=2r_0(1+\alpha_0\tau)^{1/2}/\tau$, increases with temperature. For optimally doped Bi-2212,[43–46] we have $T_{c0}\simeq 100$ K, $\Delta T_m\simeq 1$–2 K, $\alpha_0=T_{c0}/\Delta T_m=45$–90, $T=77$ K, and $\tau=1/7$; we obtain $L_n\simeq(100$–$140)r_0\approx 50$–70 Å. As above, $L_n(T)$ may increase due to the local nonstoichiometry near GB's.

Using Eq. (11), we can estimate the critical angle $\theta_n=2\sin^{-1}(b/2L_n)$, above which the normal parts of the NC core regions of neighboring dislocations start overlapping:

$$\theta_n=2\sin^{-1}\frac{\pi(1-\sigma)(T_{c0}-T)}{C(1-2\sigma)\sqrt{1+\alpha_0\tau}}. \quad (12)$$

For 77 K and the numbers used above, this yields $\theta_n(77\ \mathrm{K})\simeq 3°$–5°, in agreement with the observed onset of the sharp drop in $J_c(\theta)$.[1–7] By contrast, the dielectric parts of the NC core regions may start overlapping at a much higher angle θ_c than θ_n. Using Eq. (8), we can estimate the critical angle $\theta_c=2\sin^{-1}(b/4r_i^+)$ as follows:

$$\theta_c=2\sin^{-1}\frac{2\pi(1-\sigma)T_{c0}}{C(1-2\sigma)(1+\sqrt{1+\alpha_0})}. \quad (13)$$

For $C\simeq 300$ K, $T_{c0}\simeq 90$ K, and $\Delta T\simeq 1$–2 K, we obtain from Eq. (13) that $\theta_c\simeq 30°$–40°.

B. Electron screening in GB's

The strain decay length $d/2\pi\simeq b/2\pi\theta$ becomes smaller than $b\approx 4$ Å at comparatively small angles $\theta>9°$, for which additional mechanisms can contribute to the suppression of superconductivity near GB's. We consider here a local redistribution of the carrier density $n(x,y)$ and the shift of the chemical potential μ at the GB's which both strongly affect T_c in HTS's. If $\epsilon(x,y)$ varies over scales shorter than the Debye screening length $l_D=[\kappa_\infty/4\pi e^2N(E_F)]^{1/2}$, the local electroneutrality assumed in the previous section becomes invalid. Here $\kappa_\infty\simeq 20$–30 is the dielectric constant of the ionic lattice of HTS's,[58] $N(E_F)$ is the density of states on the Fermi surface, and $-e$ is the electron charge. Unlike low-T_c superconductors, HTS's have l_D comparable to the coherence length ξ_0,[55,56] and so the charge effects are essential, if the width of current channels in GB's becomes smaller than $2l_D$.

For an ideal electron gas in layered materials, the in-plane screening length l_D is independent of the electron density,[57] with $l_D=(\kappa_\infty s r_B)^{1/2}/2$ for $s\ll\kappa_\infty r_B$ and $l_D=\kappa_\infty r_B/2$ for $s\gg\kappa_\infty r_B$. Here $r_B=\hbar^2/me^2$ is the Bohr radius, m is the in-plane effective mass, and s is the interlayer spacing. For HTS's, the characteristic values of $l_D=5$–10 Å (Ref. 56) become larger than the strain decay length $b/2\pi\theta$ for $\theta>4°$–7°. For higher θ, the sizes of the NC core regions are smaller than the thickness $2l_D$ of the space charge layer near GB's; and thus the suppression of Δ on GB's is mostly due to the electrostatic potential $\Phi(x)$ near GB's.

We describe screening around the GB dislocations in the normal state,[63] using the Thomas-Fermi equation

$$\nabla^2\Phi-\Phi/l_D^2=-4\pi Ze\,\delta N(x,y)/\kappa_\infty, \quad (14)$$

where Ze is the ion charge and $\delta N(x,y)$ is the perturbation of the total ion density N_0 caused by the GB strains. Notice that for a two-dimensional (2D) ideal electron gas, the nonlinear corrections to Eq. (14) are absent.[57]

The atomic structure of the GB's in layered HTS's can be very complicated, since it depends not only on θ, but also on the way the different ions in adjacent crystalline lattices are matched on GB's.[29] However, the important qualitative feature of the GB structure is that it has an excess ion charge Q which is screened by electrons (holes). We calculate Q for low-angle GB's, for which we can use the continuous elasticity theory for the GB dislocations, and thus express the excess ion density at the GB's in terms of measured macroscopic parameters. To do so, we consider the simplest isotropic expansion of $\delta N(x,y)$ in *elastic* strain $\epsilon(x,y)$,

$$\delta N = -N_0(\epsilon + \zeta\epsilon^2). \tag{15}$$

Here the linear term in ϵ describes the periodic ion density variation in elasticity theory which gives zero charge after averaging along GB's. The quadratic term describes the first anharmonic correction, where ζ is the Grüneisen parameter which determines the thermal expansivity and is usually about 2 above 20–30 K.[59,60] Although small, as compared to the linear term in Eq. (15), the quadratic term is important, since it has a nonzero mean value $Q=-N_0Ze\zeta\int\langle\epsilon^2\rangle dx$ which gives the excess ion charge per unit area of GB's due to reduced ion density in the layer of thickness $d/2\pi$ near GB's:

$$Q = -\zeta eZN_0\int_{-\infty}^{\infty}\sum_G |\epsilon(k,G)|^2\frac{dk}{2\pi}$$

$$= -\frac{\zeta ZeN_0(1-2\sigma)^2b^2}{16\pi d(1-\sigma)^2}\ln\frac{d}{r_i}, \tag{16}$$

where the Fourier component $\epsilon(k,G)$ was taken from Appendix B. The total ion charge $Q(\theta)$ increases approximately linear with the GB dislocation density, $b/d\propto\sin(\theta/2)$. The nonzero Q results in a uniform shift of the mean $\Phi(x)$ which decays across GB's on the screening length l_D which is larger than $d/2\pi$ in the crucial region of intermediate θ.

It is convenient to write Φ as $\Phi=\Phi_1+\Phi_2$, where Φ_1 and Φ_2 are determined by the linear and quadratic terms in $\delta N(\epsilon)$, respectively. The solution of Eq. (14) for $\Phi_1(x,y)$ obtained in Appendix B has the form

$$\Phi_1(x,y)=\Phi_a\sum_{G>0}[e^{-|x|G}-Ge^{-|x|G_0}/G_0]\sin Gy, \tag{17}$$

where $\Phi_a=-2\pi N_0Zeb(1-2\sigma)l_D^2/d(1-\sigma)\kappa_\infty$, $G=2\pi n/d$, $G_0=(G^2+l_D^{-2})^{1/2}$, and $n=0,\pm1,\pm2,\ldots$. Here $\Phi_1(x,y)$ oscillates along GB's and exponentially decays across GB's on the lengths $d/2\pi n$. Therefore, the screening effects in the first order in ϵ only renormalize the size of the NC regions calculated in the previous section, since the fluctuation of the carrier concentration $\delta n(x,y)=-\Phi_1(x,y)/4\pi l_D^2e$ varies on the same spatial scales as the lattice strains $\epsilon(x,y)$.

The oscillations of $\delta n(x,y)$, along GB's also result in a uniform suppression of the local T_c near GB's. For the parabolic dependence $T_c=T_{cm}-A(n-n_m)^2$, the uniform shift of the critical temperature $\delta T_c(x)=T_c(x)-T_{c0}$ along GB's is given by $\delta T_c=-A\langle\Phi_1/4\pi l_D^2e\rangle^2$, where $\langle\ \rangle$ stands for spatial averaging over y. In GL theory the suppression of Δ near GB's is determined by the dimensionless parameter $\Gamma_1=-\int\delta T_c(x)dx/\xi_0T_{c0}$ (see below) which can be obtained from Eq. (17) in the form

$$\Gamma_1=\frac{A\Phi_a^2}{2T_{c0}\xi_0}\sum_{G>0}\frac{(2+g)\sqrt{1+g}+g^2-2g-2}{G(1+g)^{3/2}(1+\sqrt{1+g})}, \tag{18}$$

where $g=(l_DG)^{-2}$. For $\theta>b/2\pi l_D$, that is, $g\ll1$, the expression under the sum in Eq. (18) reduces to $5/8l_D^4G^5$. Since Φ_a in Eq. (18) is proportional to $1/d$, the parameter $\Gamma_1\propto d^3\propto1/\theta^3$ rapidly decreases with θ. Therefore, the first linear term in Eq. (15) due to elastic strains cannot give rise to any progressive depression of Δ on GB's with θ.

By contrast, the anharmonic contribution $\Phi_2(x,y)$ contains a nonoscillating term which decays over l_D across GB's and describes a shift of the mean electrostatic potential $\Phi(x)=\langle\Phi_2(x,y)\rangle$ due to the excess ion charge on GB's. As shown in Appendix B, $\Phi(x)$ is given by

$$\Phi(x)=-Fl_D^2\sum_{G>0}^{G_m}\frac{2Gl_De^{-|x|/l_D}-e^{-2|x|G}}{(2l_DG)^2-1}, \tag{19}$$

where $F=\pi eZN_0\zeta b^2(1-2\sigma)^2/2d^2(1-\sigma)^2\kappa_\infty$. Since the sum (19) diverges logarithmically at large G, we introduced a cutoff $G_m\sim2\pi/r_i$ determined by the size r_i of the dielectric core region, where Eq. (14) becomes invalid. For $\theta>b/2\pi l_D$, the second term in the numerator of Eq. (19) can be neglected, and $\Phi(x)$ takes the form

$$\Phi(x)=\Phi_0\exp(-|x|/l_D), \tag{20}$$

where Φ_0 to logarithmic accuracy is given by

$$\Phi_0\simeq-\frac{eZN_0\zeta b(1-2\sigma)^2l_D\ln(d/r_i)}{4(1-\sigma)^2\kappa_\infty}\sin\frac{\theta}{2}. \tag{21}$$

The amplitude Φ_0 increases approximately linear with θ for $\theta\ll1$. Taking for $YBa_2Cu_3O_7$,[56,62] $\sigma=0.25$, $ZN_0=n_0=5\times10^{21}$ cm^{-3}, and $\kappa_\infty=20$, we obtain $e\Phi_0\sim6$ meV for $d=4b=4r_i$, $\theta=20°$, $l_D=8$ Å, $\zeta=2$.

The 2D isotropic equation (14) gives the simplest self-consistent description of charge effects near GB's, although it does not take into account all characteristic features of the electron band structure of HTS's and nonlocal electron screening. The nonlocality increases the effective screening length for charge fluctuations with the wave vector k comparable to the 2D Fermi wave vector $k_F\simeq(2\pi n_0s)^{1/2}$.[57] Due to the low carrier density n_0, the condition $k\sim2\pi/d\sim k_F$ is characteristic of GB's in HTS's, resulting in the effective screening length l_D which can substantially exceed its Thomas-Fermi value. Thus, the electric potential $\Phi(x)$ near GB's becomes more long range, varying on lengths of the order of the mean spacing between carriers $\sim n_0^{-1/3}$ which is about 6 Å for optimally doped $YBa_2Cu_3O_7$ ($n_0\simeq5\times10^{22}$ cm^{-3}). We do not consider here the more complicated nonlocal screening near GB's, restricting ourselves to a qualitative description in the framework of the Thomas-

Fermi approach with an effective l_D extracted from observed strong electric field effects in HTS's which indicate that $l_D \simeq 5-10$ Å.[56]

The nonlocality also makes $\Phi(x)$ dependent on details of the electron band structure of HTS's, such as the extended saddle point singularities near the Fermi level and planar portions on the Fermi surface along the [100] and [010] directions in the Brillouin zone.[64–67] For $s \gg \kappa_\infty r_B$, the screened potential $\Phi(x,y)$ is long range[57] ($\Phi \propto 1/r^3$) and also exhibits Friedel's oscillations,[63,59]

$$\Phi(x) \propto \frac{c_0 \cos Qx}{|x|} e^{-|x|/\xi_1}, \quad Q|x| > 1, \tag{22}$$

along the a or b axes. Here Q is the nesting wave vector between the neighboring planar portions of the Fermi surface, which is $Q \approx 0.3$ Å^{-1} for optimally doped HTS's.[64–66] This gives the period of the oscillations, $l_f = 2\pi/Q \simeq 20$ Å. The factor $\exp(-|x|/\xi_1)$ accounts for the damping of the Friedel oscillations in the superconducting state, where $\xi_1(T)$ weakly depends on temperature and approximately equals the superconducting coherence length $\xi(0)$ at $T=0$.[68,69] Impurities do not affect the Friedel oscillations, if the electron mean free path l_i is much larger than ξ_0. The case $l_i > \xi_0$ is characteristic of HTS materials which usually correspond to the clean limit $\xi_0 \ll l_i$. Therefore, the length $l_D \sim \xi_1 \simeq 10-15$ Å can be regarded as an intrinsic effective thickness over which the order parameter is depressed near the GB's.

C. Heterogeneity scales of the T_c suppression on GB's

Now we consider how the heterogeneity of the GB's can affect superconducting properties. The NC regions, spaced by d, consist of an insulating domain of size $2r_i$ surrounded by metallic shell in which the *local* superconducting coupling constant λ is suppressed on the scale of a few atomic spacings. Below T_c, these small metallic core regions ($r^+ < \xi$) become superconducting due to the proximity effect and therefore transparent to the transport current. However, the dielectric core regions are not affected by the proximity effect and remain stronger barriers for the current flow. For the ideal GB's shown in Fig. 1, the size r_i calculated above in the linear elasticity theory decreases with θ due to the compensation of strain fields in GB's as d decreases (see Appendix A). However, if $r_i(\theta)$ becomes comparable with b, the decrease of r_i is limited by plastic effects near dislocation cores.[22,72] The local suppression of Δ on GB's due to the NC regions is determined by the parameter[42]

$$\Gamma_1 \sim \frac{L_n^2}{d\xi_0} \propto \sin\frac{\theta}{2}, \tag{23}$$

which is a fraction occupied by the normal NC regions in the layer of thickness ξ_0 near GB's. These normal regions give rise to the proximity effect suppression of Δ linear in the GB dislocation density.

For $\theta > b/2\pi l_D$, the NC regions become smaller than the screening length l_D; thus the superconductivity suppression on GB's is mostly due to the shift Φ_0 of the averaged electrical potential on GB's. This results in the opposite shift of the chemical potential μ by $\mu_0 = -e\Phi_0$ to provide a constant electrochemical potential $\mu_e = \mu + e\Phi$. However, T_c of HTS's is generally quite sensitive to small shifts of μ, since comparatively small changes of the in-plane hole concentration c can cause the transition into an insulating antiferromagnet[50] (see Fig. 3). Due to the small Fermi energy in HTS's, $E_F \sim 0.1$ eV, the above-estimated shift of μ on GB's by $e\Phi \sim 5-10$ meV$\sim T_c$ appears to be of the order of the change of μ which can cause strong local suppression of Δ.[50,67,70,71]

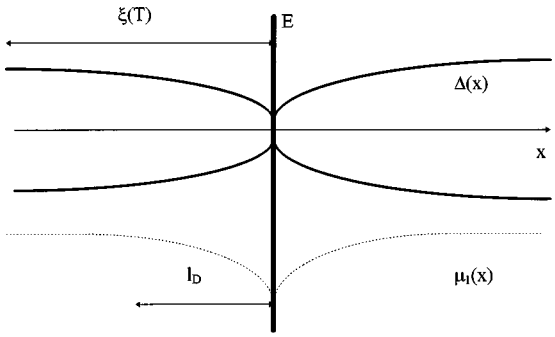

FIG. 5. Suppression of the order parameter near GB's due to the variation of the chemical potential in the layer of thickness $2l_D < \xi(T)$. The dashed curve depicts the energy of the extended saddle point singularity in $N(E)$.

These qualitative estimates indicate that the charge effects can provide a universal mechanism of the local superconductivity suppression on GB's. This mechanism is amplified by the extended saddle point singularities in the HTS electron density of states $N(E)$ observed in photoemission experiments at energies $E = -\mu_1 \approx 20-30$ meV below the Fermi level.[64–67] The resulting singularity in $N(E)$ near the Fermi surface not only can enhance the bulk T_c,[70,71] but also can make T_c sensitive to any shifts of μ of order μ_1. Since $e\Phi_0$ on GB's turns out to be comparable to the μ_1, the shift of the peak in $N(E)$ away from its presumably optimum position at μ_1 can further suppress Δ in the layer of thickness $2l_D$ around GB's, as shown in Fig. 5.

We estimate the suppression of $\Delta(x)$ due to the local variations of $\Phi(x)$ in GL theory which has been used to describe $\Delta(x,y)$ near various structure defects for both s- and d-wave symmetries of the order parameter[74] and in the presence of extended saddle point singularities.[71] We illustrate here the essential physics by the simplest s-wave GL equation, since $J_c(\theta)$ calculated below turns out to be only weakly sensitive to the symmetry of Δ in the region of small θ. The GL equation with a locally nonuniform superconducting coupling constant $\lambda(\mathbf{r})$ has the form[73]

$$\xi_0^2 \nabla^2 \Delta + \left[\ln\frac{T_c(\mathbf{r})}{T} - \frac{\Delta^2}{\Delta_0^2} \right] \Delta = 0. \tag{24}$$

Here ξ_0 and Δ_0 are of the order of the zero-temperature coherence length $\xi(T) = \xi_0/\sqrt{\tau}$ and the gap $\Delta(T) = \sqrt{\tau}\Delta_0$, respectively, and $\tau = (T_{c0} - T)/T_{c0} \ll 1$ near the bulk T_{c0}. The value $\xi_0 = (\phi_0/2\pi H'_{c2} T_c)^{1/2}$ can be extracted from the observed temperature derivative of the upper critical field H'_{c2} at T_c, giving $\xi_0 \approx 13$ Å for $YBa_2Cu_3O_7$ ($T_c = 90$ K, $H'_{c2} \approx 2$ T/K). Taking the BSC-type dependence T_c

$=\omega_0\exp(-1/\lambda)$ and assuming that T_c is mostly determined by the local depression of λ near GB's, we can rewrite Eq. (24) in the form

$$\xi_0^2\nabla^2\Delta+\left[\tau-\frac{\Delta^2}{\Delta_0^2}\right]\Delta=\left[\frac{1}{\lambda(\mathbf{r})}-\frac{1}{\lambda_\infty}\right]\Delta, \tag{25}$$

where λ_∞ is the coupling constant away from GB's. The right-hand side of Eq. (25) describes the localized perturbation $V(\mathbf{r})\Delta$ due to the suppression of $\lambda(\Phi)$ near GB's. Assuming a smooth dependence of λ on μ, we get $V(x)=-e\Phi(x)(\partial\lambda_\infty/\partial\mu)/\lambda_\infty^2$, if $e\Phi_0(\theta)$ is smaller than the critical shift of the chemical potential μ_c which causes the superconductor-insulator transition. Since Φ_0 on GB's increases with the dislocation density, this mechanism provides the progressive decrease of Δ on GB's with θ, which, in turn, gives rise to the rapid decrease of $J_c(\theta)$ considered in the next section. The angular dependence $J_c(\theta)$ is thus determined by the domelike dependence $\lambda(\mu)$ characteristic of HTS's.

Therefore, besides the spacing between the GB dislocations, there are two additional intrinsic length scales associated with GB's. The first one is the size $r_i\simeq b$ of the insulating core regions which provide strong barriers for current flow. The second scale is the width $2l_D$ of a layer of suppressed Δ across GB's which is determined by the charge effects.

III. CRITICAL CURRENT

Now we calculate J_c for a uniform current flowing perpendicular to GB's, by solving the GL equation

$$\xi^2\nabla^2\psi+\psi-\psi^3-\frac{i^2}{\psi^3}=V(\psi,\mathbf{r}), \tag{26}$$

where $\psi=\Delta/\Delta_b$ is the order parameter normalized to its bulk value $\Delta_b=\Delta_0\sqrt{\tau}$, $i=J/J_0$ is the dimensionless transport current density away from GB's, $J_0=c\phi_0/16\pi^2\lambda_L^2\xi$ is of the order of the depairing current density, and $\lambda_L(T)=\lambda_{L0}/\sqrt{\tau}$ is the London penetration depth.

The left-hand side of Eq. (26) is the usual GL equation in the presence of uniform current,[73] and the right-hand side describes the perturbation caused by GB's,

$$V=\frac{1}{\tau}\left[\frac{1}{\lambda(\mathbf{r})}-\frac{1}{\lambda_\infty}\right]\psi+\frac{i_0^2(\mathbf{r})-i^2}{\tau\psi^3}, \tag{27}$$

where $i_0(\mathbf{r})$ is the normalized current density near GB's, where both $i_0(\mathbf{r})$ and $\lambda(\mathbf{r})$ are strongly inhomogeneous due to the local T_c suppression and the channel structure of GB's. The first term on the right-hand side of Eq. (27) describes the local T_c suppression across the GB's and the modulation of $\Delta(x,y)$ along GB's caused by the NC regions. The second term in Eq. (27) results from the decrease of the GB current-carrying cross section by the insulating parts of the NC regions. This gives rise to a local concentration of $j(x,y)$ in the current channels, which further depresses Δ.

Equation (26) describes the distribution of $\Delta(x,y)$ for the proximity coupled NC regions. The general case of $d>\xi(T)$ is very complicated; however, the situation simplifies if the effective GB thickness $l_0=2l_D$ and the dislocation spacing d are much smaller than $\xi(T)$ [which corresponds to $\theta>b/\xi(T)\sim 5^\circ$ for $YBa_2Cu_3O_7$ at 77 K]. In this case the particular shape of the NC regions becomes less essential, because $\Delta(x,y)$ is mostly determined by $V(x,y)$ averaged along GB's.[42] Since $l_D\ll\xi(T)$ near T_c, the localized potential $V(x,y)$ can be written as

$$V=V_0\delta(x),\quad V_0=\int_{-\infty}^{\infty}\langle V(x,y)\rangle dx, \tag{28}$$

where $\langle\cdots\rangle$ stands for the spatial averaging along GB's, and $\delta(x)$ is the delta function. It is convenient to rewrite Eq. (26) in the following dimensionless form:

$$\psi''+\psi-\psi^3-i^2/\psi^3-\Gamma(\psi,i)\,\delta(\eta)=0, \tag{29}$$

where the prime denotes differentiation with respect to $\eta=x/\xi(T)$ and $\Gamma(\psi,i)=V_0(\psi,i)/\xi(T)$. Equation (29) can be solved exactly for any dependence $\Gamma(\psi)$.[75] The solution $\psi(\eta)$ obtained in Appendix C has the form

$$\psi^2(\eta)=\psi_m^2+(\psi_\infty^2-\psi_m^2)\tanh^2\left[\frac{(|\eta|+\eta_0)\sqrt{\psi_\infty^2-\psi_m^2}}{\sqrt{2}}\right]. \tag{30}$$

Here ψ_∞ and ψ_m are given by

$$i^2=\psi_\infty^4(1-\psi_\infty^2),\quad \psi_m^2=2i^2/\psi_\infty^4. \tag{31}$$

The first equation in Eq. (31) describes the suppression of ψ by uniform current,[73] and η_0 is defined by $\psi(0)=\psi_0$. The order parameter ψ_0 on GB's satisfies the following equation:

$$2E-\psi_0^2+\frac{\psi_0^4}{2}-\frac{i^2}{\psi_0^2}=\frac{\Gamma^2(\psi_0)}{4}, \tag{32}$$

where $E=\psi_\infty^2-3\psi_\infty^4/4$. For $i=0$, Eqs. (27), (31), and (32) yield $\Gamma(\psi)=\Gamma_1\psi$, $\psi_\infty=1$, $\psi_m=0$, and

$$\eta_0=\sqrt{2}\,\tanh^{-1}\left(\sqrt{1+\frac{\Gamma_1^2}{8}}-\frac{\Gamma_1}{2\sqrt{2}}\right). \tag{33}$$

The distribution $\psi(x)$ described by Eqs. (30) and (33) is shown in Fig. 6, where $\psi_0=1-\Gamma_1/2\sqrt{2}$ at $\Gamma_1\ll 1$, and $\psi_0=\sqrt{2}/\Gamma_1$ for $\Gamma_1\gg 1$.

For a qualitative analysis of $\psi(x,i)$ at $i>0$, it is convenient to use an analogy of Eq. (29) with the equation that describes the classical motion of a particle of the unit mass and energy E in the potential

$$U(\psi)=\frac{\psi^2}{2}-\frac{\psi^4}{4}+\frac{i^2}{2\psi^2}, \tag{34}$$

where ψ and η play the role of the particle coordinate and time, respectively. The term $\Gamma(\psi)$ in Eq. (29) describes an elastic reflection of the particle at $\psi=\psi_0$. We seek a symmetric trajectory $\psi(\eta)$ of the particle which starts moving from point b with an infinitesimal velocity and $\psi=\psi_\infty$, then gets reflected at $\psi=\psi_0$, and comes back to b with zero velocity. The graphic solution of Eq. (32) for ψ_0 is shown in Fig. 7, where ψ_0 corresponds to the intersection points of the

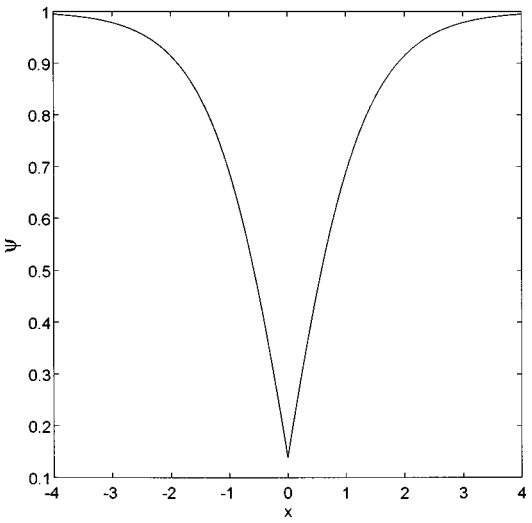

FIG. 6. Distribution $\psi(\eta)$ near GB's described by Eqs. (30) and (33) for $i=0$ and $\Gamma_1=10$. The coordinate x is normalized by $\xi(T)$.

curves $-\Gamma^2(\psi)/4$ and $U(\psi)-E$. As seen from Fig. 7, Eq. (32) has several roots, of which only those with $d\psi_0/di<0$ are stable.[75] The only stable solution s in Fig. 7 disappears at $i>i_c$, where i_c determines the critical current density through GB's which is basically the depairing current density for the self-consistent distribution (30).

Now we consider $\Gamma(\psi)$ which follows from Eq. (27):

$$\Gamma(\psi)=\Gamma_1\psi+\Gamma_2 i^2/\psi^3. \tag{35}$$

The parameter Γ_1, which describes the local suppression of T_c on GB's, increases with θ due to the domelike dependence of the superconducting coupling constant $\lambda[\mu+e\Phi(\theta)]$ in HTS's on the chemical potential. We do not discuss here specific dependences $\lambda(\mu)$ for various microscopic models published in the literature, focusing instead on a phenomenological description of $J_c(\theta)$ which can be obtained by expanding $\lambda\simeq\lambda_\infty+(\partial\lambda_\infty/\partial\mu)e\Phi_0$ in Eq. (27) for small $e\Phi_0$. This gives Γ_1 which increases approximately linearly with the GB dislocation density:

$$\Gamma_1=\frac{2l_D e\Phi_m}{\lambda_\infty\mu_c\xi_0\sqrt{\tau}}\sin\frac{\theta}{2}. \tag{36}$$

Here $\mu_c=|\partial ln\lambda_\infty/\partial\mu|^{-1}$ is of the order of the shift of μ which causes the S-I transition, and the amplitude Φ_m is defined by $|\Phi_0(\theta)|=\Phi_m\sin(\theta/2)$, where $\Phi_0(\theta)$ is given by Eq. (21). The nonlinearity of the function $T_c(\mu)$ could be taken into account by assuming the conventional parabolic dependence $T_c(x)=T_{c0}[1-a_1\Phi(x)-a_2\Phi^2(x)]$ in Eq. (24), where $a_{1,2}$ are constants. This results in a nonlinear and fairly cumbersome dependence of $\Gamma_1\propto\int\ln(T_c/T_{c0})dx$ on $\sin\theta$ which we do not consider here, since the much simpler Eq. (36) based on the linear expansion of $\lambda(\mu)$ already provides a good description of the observed $J_c(\theta)$ (see below).

The parameter Γ_2 in Eq. (35) accounts for the decrease of the current-carrying cross section of GB's by the insulating NC regions. In this case the local current density is enhanced in the superconducting channels between the dislocation

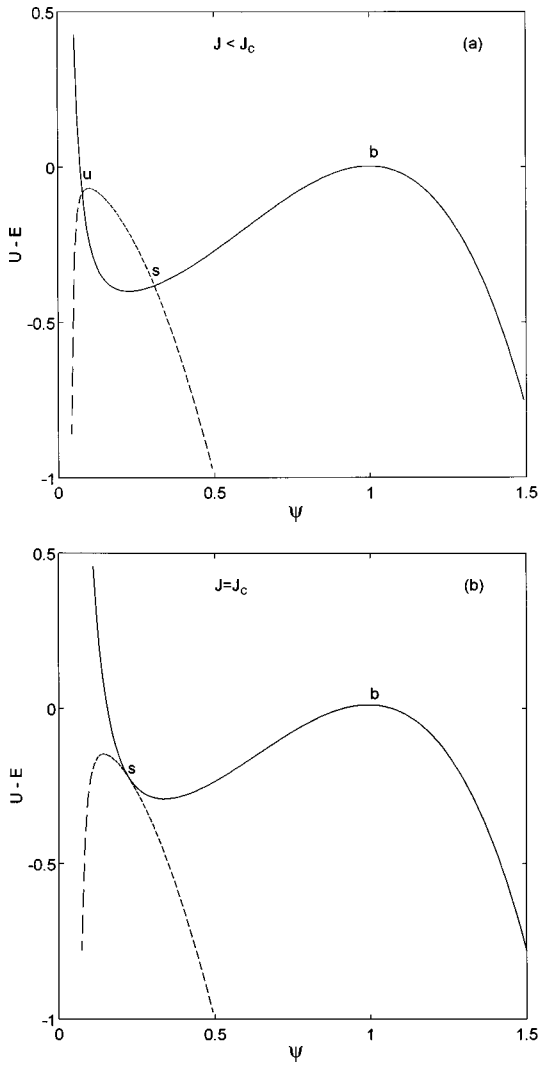

FIG. 7. Graphic solution of Eq. (32) for $J<J_c$ (a) and $J=J_c$ (b). The particle of energy E moves in the potential $U(\psi)$, reflecting in the intersection points of $U(\psi)-E$ (solid curve) and $-\Gamma^2(\psi)/4$ (dashed curve).

cores and in the layer of thickness $\simeq 4r_i$ around GB's, where r_i is an effective radius of the NC regions. Then Γ_2 can be written in the form

$$\Gamma_2=\frac{4r_i}{\xi_0\sqrt{\tau}}\left[\frac{d^2}{(d-2r_i)^2}-1\right]=\frac{4r_i\nu(2-\nu)}{\xi_0\sqrt{\tau}(1-\nu)^2}. \tag{37}$$

Here the term $d^2/(d-2r_i)^2$ describes the local enhancement of i^2 in the current channels, and

$$\nu=\frac{\sin(\theta/2)}{\sin(\theta_c/2)}, \tag{38}$$

where θ_c is the critical angle, $\theta_c=2\sin^{-1}(b/4r_i)$ at which the insulating NC regions overlap.

For arbitrary Γ_1, Γ_2, the critical current i_c is determined by two cumbersome algebraic equations for $\psi_0(i)$ and i_c. A simpler case $\Gamma_2=0$, $\Gamma_1>0$ corresponds to a uniform Josephson contact with suppressed order parameter, for which J_c is determined by a single algebraic equation given in Appendix C [numerical simulation of Eqs. (29) and (35) for

$\Gamma_2=0$ was performed by Campbell[36]. Hereafter we focus on the most interesting case $\Gamma_1 \gg 1$, $\Gamma_2>0$, for which a GB exhibits weak-link behavior. As follows from Eq. (36), the condition $\Gamma_1 \gg 1$ does hold, since $2l_D \simeq \xi_0$, $\tau \ll 1$ and $e\Phi_0/\lambda_\infty \mu_c > 1$ for weak coupling. If $\Gamma_1 \gg 1$, then $i^2 \ll 1$, and so we can put $\psi_\infty^2 = 1-i^2$ and $\tanh^2(\eta_0/\sqrt{2}) = \psi_0^2 - 2i^2$ in Eqs. (30) and (31). In this case Eq. (32) reduces to (see Appendix C):

$$u^4 - 2u^3 + 2qu^2 + \alpha^2 q^2 = 0, \tag{39}$$

$$\alpha = \frac{\Gamma_1\Gamma_2}{2+\Gamma_1\Gamma_2}, \quad q = (2+\Gamma_1\Gamma_2)\Gamma_1^2 i^2, \tag{40}$$

where $u=\psi_0^2$. A graphic analysis of Eq. (39) similar to that in Fig. 7 shows that the stable solution $u_s(q)$ exists only below the critical value $q<q_c$ which determines J_c. At $q=q_c$ points s and u in Fig. 7 merge at $u=u_c$, and the stable solution disappears, if $q>q_c$. The value u_c can be found by differentiating Eq. (39) with respect to u, giving $q_c = u_c(3/2-u_c)$. Substituting this q_c into Eq. (39) and solving a quadratic equation for $u_c(\alpha)$, we calculate $q_c = u_c(3/2-u_c)$ and finally obtain J_c in the following scaling form:

$$J_c = \frac{J_m}{\nu}\left[\frac{1-9\alpha^2+(1+3\alpha^2)^{3/2}}{(1+\alpha)(1-\alpha^2)}\right]^{1/2}, \tag{41}$$

$$J_m = \frac{J_0 b\sqrt{\tau}}{2\sqrt{2}\beta\xi_0 \sin(\theta_c/2)}, \tag{42}$$

$$\alpha = \frac{\beta\nu^2(2-\nu)}{2\tau(1-\nu)^2+\beta\nu^2(2-\nu)}. \tag{43}$$

Here the dependence of α on ν and τ was found, using Eqs. (36), (37), and (40). The control parameter $\beta = 2l_D be\Phi_m/\xi_0^2\mu_c\lambda_\infty$, which determines how fast $J_c(\theta)$ decreases with θ, can be obtained from Eq. (21):

$$\beta = \frac{e^2 n_0 \zeta \ln(b/r_i\theta)}{2\kappa_\infty\mu_c\lambda_\infty}\left[\frac{bl_D(1-2\sigma)}{\xi_0(1-\sigma)}\right]^2. \tag{44}$$

Notice that for $\Gamma_1 \gg 1$, the parameter Γ_2 enters Eq. (41) only in the combination $\Gamma_1\Gamma_2$, and so even a weak blockage of current by the NC core regions ($\Gamma_2 \ll 1$) can markedly suppress J_c, if $\Gamma_1\Gamma_2 > 1$. For $\Gamma_1\Gamma_2 \gg 1$, Eq. (41) yields

$$J_c = \frac{3\sqrt{3}J_0}{8\Gamma_1\sqrt{\Gamma_1\Gamma_2}} = J_1\frac{\tau^{5/2}(1-\nu)}{\nu^2(2-\nu)^{1/2}}, \tag{45}$$

$$J_1 = \frac{3\sqrt{3}bJ_0(0)}{8\beta^{3/2}\xi_0 \sin(\theta_c/2)}, \tag{46}$$

where $J_0(T) = J_0(0)\tau^{3/2}$. The suppression of J_c due to the current channels manifests itself in the additional factor $\sqrt{\Gamma_1\Gamma_2} > 1$ in Eq. (45), as compared to $J_c \sim J_0/\Gamma_1$ for $\Gamma_2=0$ and $\Gamma_1 \gg 1$ (see Appendix C). Equation (45) corresponds to the GL temperature region $T \simeq T_c$ in which $J_c \propto \tau^{5/2}$ rapidly decreases with T and θ. The temperature dependence (45) differs from the $J_c \propto \tau$ for S-I-S Josephson contacts and is rather consistent with the observed quadratic dependence,[5,76,77] $J_c \propto \tau^2$ characteristic of S-N-S contacts.[78] In this model which neglects the Josephson tunneling through insulating dislocation cores, $J_c(\theta)$ vanishes at $\theta=\theta_c$. When taking into account the tunneling through the insulating NC regions at $\theta > \theta_c$, the critical current remains finite, though its angular dependence $J_c(\theta)$ might change as compared to $\theta < \theta_c$.

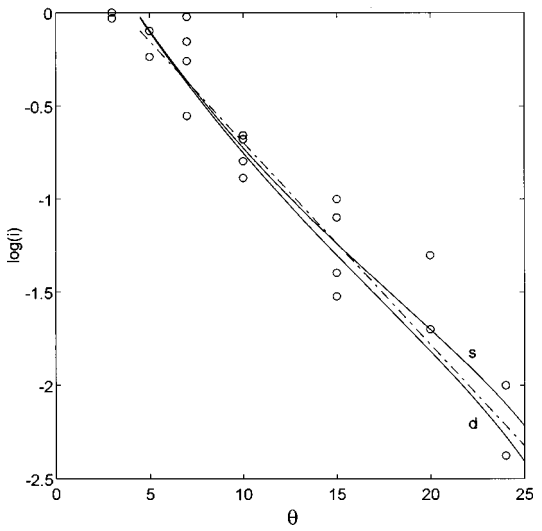

FIG. 8. Fit with the experimental data on thin film [001] tilt $YBa_2Cu_3O_7$ bicrystals with $\beta=2.7$ and $\theta_c=30°$. Curves s and d correspond to the s and d pairings, respectively. They are related by Eq. (47), where $J_c(\theta)$ for the s pairing is given by Eq. (41). The dashed line shows the function $\exp(-\theta/\theta_0)$ with $\theta_0=4°$.

IV. COMPARISON WITH EXPERIMENT AND DISCUSSION

Equation (41), which gives the explicit dependence of J_c on θ and T, contains three control parameters β, θ_c, and J_m. When comparing the calculated $J_c(\theta,T)$ with experiment, the amplitude J_m can be eliminated by normalizing $J_c(\theta)$ to its value $J_c(\theta_0)$ for a certain misorientation angle $\theta_0 \simeq 3°-5°$ at which $J_c(\theta_0)$ equals J_g in the grains. Small $\theta < \theta_0$ correspond to a plateau on the observed $J_c(\theta)$ curves in Fig. 8 in the region between θ_0 and the base data point $\log i = 0$ at $\theta=0$, where $J_c(\theta)$ values through GB's are hardly accessible in resistive experiments. Thus, we are left with two parameters $\beta \sim 1$ and $\theta_c \simeq 20°-40°$ which can be extracted from the best fit with experimental data, which are usually well described by the exponential dependence $J_c \propto \exp(-\theta/\theta_0)$ with $\theta_0 \simeq 4°-5°$. The fact that all uncertain microscopic parameters near GB's, l_D, μ_c, ζ κ_∞, and λ_∞, can be combined in a single parameter β markedly simplifies the comparison of our model with experiment.

As an illustration, Fig. 8 shows the observed $J_c(\theta)$ for $YBa_2Cu_3O_7$ bicrystals[7] at 77 K similar to analogous $J_c(\theta)$ dependences for other thin film and bulk HTS bicrystals.[1–3,5,6] Given the typical scatter of experimental data, the fit, which corresponds to $\beta=2.7$ and $\theta_c=30°$, turns out to be quite good. The algebraic function (41) describes well the apparent quasiexponential decrease of $J_c(\theta)$ by two to three orders of magnitude in the region $0<\theta<30°$. The calculated $J_c(\theta)$ also appears to be rather close to the

straight dashed line in Fig. 8 which corresponds to $J_c(\theta) = J_0\exp(-\theta/\theta_0)$ with $\theta_0 = 4°$.

So far we have not specified the symmetry of the order parameter, since the final $J_c(\theta)$ dependence is in fact only weakly sensitive to the symmetry of Δ at $\theta < \theta_c$. For instance, the $J_c^{(d)}(\theta)$ for d-wave pairing is related to the s-wave $J_c^{(s)}(\theta)$ as follows:

$$J_c^{(d)}(\theta) = \cos^2 2\theta J_c^{(s)}(\theta), \tag{47}$$

where the factor $\cos^2 2\theta$ accounts for the matching conditions of the superconducting d-wave gap function on GB's.[9,80] Equation (47) also implies that the gap suppression on GB's is weakly sensitive to the symmetry of the order parameter, as was assumed by Hilgenkamp *et al.*[10] As follows from Fig. 8, the factor $\cos^2(2\theta)$ only gives a relatively small correction to the much stronger decrease of $J_c(\theta)$ caused by the local superconductivity suppression near GB's.

Since Eq. (41) describes well the observed angular dependence $J_c(\theta)$, we can independently check the self-consistency of the model by comparing the absolute value of J_c given by Eq. (45) with experiment. Likewise, the parameter β extracted from the fit can be compared with what follows from Eq. (44). For $\beta = 2.7$, $\theta_c = 30°$, $b = 4$ Å, $\xi_0 = 13$ Å, $\lambda_{L0} = 1500$ Å, $\tau = 1/7$, and $\theta = 15°$, we obtain, from Eqs. (45) and (46), that $J_c \sim 2\times 10^5$ A/cm^2, in agreement with typical observed J_c values for [001] 15° tilt $YBa_2Cu_3O_7$ thin film bicrystals at 77 K.[3,6,7] In order to evaluate β, we take $d = 4b = 4r_i$, $\theta = 5°$, $l_D = 8$ Å, $\xi_0 = 13$ Å, $\sigma = 0.25$, $\zeta = 2$, and $n_0 = 5\times 10^{21}$ cm^{-3}. Then Eq. (44) gives $\beta = 2.7$ for $\lambda_\infty \mu_c \simeq 9$ meV$\simeq T_c$. For the 15° GB, the d-wave correction in Eq. (47) reduces J_c by 25%.

The critical angle θ_c lies in the region 20°–40°, if $r_i \simeq b$ [see Eq. (13)]. A more accurate estimate for θ_c is hard to obtain, not only because the detailed shape of the NC core regions is sensitive to the local parameters near GB's which are not well known, but also because θ_c depends on the atomic structure of the plastically deformed and compositionally different dislocation cores in HTS's.[24–29] However, the dependence (41) is only weakly affected by the uncertainty in θ_c, if θ is not too close to θ_c. The parameter β which determines the superconductivity suppression on GB's, increases for layered HTS materials which have a low carrier density, short coherence length ξ_0, and large screening length l_D. Notice that the local superconducting properties on GB's are determined not only by atomic displacements near GB's seen by electron microscopy,[24–29] but rather by the resulting variations of the local density of states $N(E_F,\mathbf{r})$ along the GB's. The variations of $N(E_F,\mathbf{r})$ could be revealed by scanning tunnel microscopy, thus providing very important information on the electron structure of the insulating NC regions and the space charge layer near GB's.

In this paper we considered the region of high temperatures $T_c - T \ll T_c$, in which many uncertainties of microscopic mechanism of high-T_c superconductivity can be effectively treated by the universal GL equations. The description of GB's at lower temperatures is more model dependent and requires much more complicated Eilenberger's or Bogolubov–de Gennes equations.[79–81] However, the similarity in $J_c(\theta,T)$ dependences observed on GB's at high and low temperatures allows us to assume that our model may give a qualitative description of the low-T region as well. Yet there are new features characteristic of the d-wave symmetry of Δ, such as localized zero-energy electron states at the S-I interface, which may contribute to the tunneling J_c of Josephson contacts in anisotropic HTS's.[79]

When calculating J_c, we assumed uniform current flow through GB's which is characteristic of thin film bicrystals of thickness L_z much smaller than the Josephson penetration depth $\lambda_J = (c\phi_0/16\pi^2\lambda_L J_c)^{1/2}$, where c is the speed of light and ϕ_0 is the flux quantum. For bulk bicrystals, with $L_z \gg \lambda_J$, the transport current only flows in the peripheral layer of thickness λ_J, and so the total critical current through GB's equals $I_c = P\lambda_J J_c$, where P is the perimeter of the GB's.[82] Thus the mean critical current density $J_b = J_c/A$, normalized to the cross-sectional area A, is given by

$$J_b = \frac{(c\phi_0 J_c)^{1/2} P}{4\pi A\sqrt{\lambda_L}}. \tag{48}$$

Equation (48) corresponds to an isotropic superconductor. For an anisotropic slab with $A = L_y L_z$ and London penetration depths λ_{Ly} and λ_{Lz} along the y and z axes, respectively, the factor $P/A\sqrt{\lambda_L}$ should be replaced by

$$\frac{P}{A\sqrt{\lambda_L}} \to \frac{2}{L_y\sqrt{\lambda_{Lz}}} + \frac{2}{L_z\sqrt{\lambda_{Ly}}}. \tag{49}$$

The apparent J_b in bulk bicrystals depends on the sample geometry and is strongly reduced by the factor $P\lambda_J/A \ll 1$, as compared to the local J_c. At the same time, $J_b(\theta) \propto J_c^{1/2}(\theta)$ exhibits weaker dependence $J_b \propto \exp(-\theta/2\theta_0)$ than $J_c(\theta)$ at $\theta < \theta_b$, where θ_b is defined by $\lambda_J(\theta_b) \simeq \min(L_z, L_y)$. At $\theta_b \simeq \theta_b$, the slope of $\ln J_c(\theta)$ increases by 2 times, since, for $\theta > \theta_b$, current flows uniformly through GB's; and thus $J_b(\theta) \simeq J_c(\theta)$.

In our model, the strong decrease of $J_c(\theta)$ with θ is due to the excess ion charge $Q(\theta)$ of the GB dislocation structure. This was shown for the simplest anharmonic correction $\zeta\epsilon^2$ in an isotropic approximation characterized by the single constant ζ. For orthorhombic crystalline symmetry, the term $\zeta\epsilon^2$ turns into the quadratic invariant $\zeta_a\epsilon_{aa}^2 + \zeta_b\epsilon_{bb}^2 + \zeta_1\epsilon_{aa}\epsilon_{bb} + \zeta_2\epsilon_{ab}^2$ which is proportional to the elastic energy density in the Grüneisen approximation. The crystalline anisotropy somewhat complicates the above analysis, but it does not change the key point that $Q(\theta)$ increases with the GB dislocation density $b/d \propto \sin(\theta/2)$, resulting in a shift of the chemical potential and the superconductivity suppression on GB's. This was obtained in the framework of the continuous elasticity theory which can be used for low-angle GB's with $d \gg b$. The discreteness of the crystalline lattice and broken atomic bonds along GB's can affect Q for higher θ and, in principle, could result in dips in $Q(\theta)$ for certain symmetric misorientations. This might pertain to the non-weak-link behavior observed on some high-angle GB's.[83,84] The atomic displacements on GB's which give rise to the nonzero $Q(\theta)$ could also be independently obtained by scanning electron tunnel microscopy,[24,29] which would enable one to calculate $Q(\theta)$ and $J_c(\theta)$ for high-angle GB's as well.

Charge effects in HTS's have recently attracted much attention due to a possibility to affect T_c by applying strong electric field E, which can have various applications in superconducting electronics.[56] As was shown above, the significant suppression of $J_c(\theta)$ can be due to localized $E(x)$ of the charged GB dislocation structure which shifts the chemical potential on GB's as θ increases. This is similar to the suppression of the order parameter on GB's by external gate voltage in HTS transistors, resulting in a significant change of J_c of GB's observed in experiment.[56] Another indication of the importance of the charge effects on GB's follows from electromigration experiments[33] which showed a noticeable change of J_c across GB's after applying pulse electric fields at $T>T_c$. This is consistent with our model in which even subtle changes in the ionic structure on GB's due to electromigration can significantly affect Q and thus J_c.

Summarizing the obtained results, we can point out the following main factors which can contribute to the low J_c values of GB's in HTS materials.

(1) The proximity of the HTS transition to the metal-insulator transition makes the order parameter on the GB's sensitive to small shifts of the chemical potential caused by local excess ion charge on structural defects screened by electrons (holes). This can result in the strong superconductivity suppression near the GB amplified by the extended saddle point singularities in the electron density of states of HTS's.

(2) The antiferromagnetic insulating phase in the HTS phase diagram manifests itself in the insulating core regions caused by large strains near the GB dislocation cores and charge effects on the GB's. These insulating core regions are strong barriers for current flow which also significantly enhance the effect of the local superconductivity suppression in the current channels at $J>0$.

(3) The suppression of the superconducting coupling constant occurs in the double-charge layer near GB's comparable to the coherence length ξ_0. This results in a large effective thickness of the GB's, which is also specific to HTS's due to their short ξ_0 and large l_D. By contrast, GB's in low-T_c superconductors with $l_D \ll \xi_0$ are not strong barriers for current flow.

V. CONCLUDING REMARKS

In this paper we mostly focused on those general features of the current transport through low-angle GB's which are rather insensitive to the microscopic mechanism of superconductivity, the symmetry of the order parameter, and detailed structure of the dislocation core regions. Our model, which links the dependence $J_c(\theta)$ with normal properties and the phase diagram of HTS's, describes well the observed strong dependence of $J_c(\theta)$ on misorientation angle even for the simplest ideal GB dislocation structure shown in Fig. 1. The partial dislocation structure of GB's in HTS's (Ref. 31) increases the effective thickness of GB's, thus making the charge effects and the suppression of Δ on GB's more pronounced. Macroscopic inhomogeneites of GB's are due to local nonstoichiometry, faceting, and resulting long-range strain fields which can subdivide GB's into weakly coupled segments connected in parallel.[85] Though important for current percolation in polycrystalline HTS's,[13,16] the faceting can hardly change qualitatively the general quasiexponential dependence of $J_c(\theta)$ on θ which is mostly determined by the segments of GB's with maximum J_c values.

Another important issue concerns the dependence $J_c(\theta,H)$ in the magnetic field H, which is determined not only by the local current transport through GB's, but also by depinning of vortices localized on GB's. The latter depends on the change of the core structure of vortices on GB's and their magnetic interaction with strongly pinned bulk vortices.[86] Here the charge effects on GB's can also essentially contribute to the vortex pinning.[55]

ACKNOWLEDGMENTS

This work was supported by NSF MRSEC Program No. DRM 9214707. The authors are grateful to D.C. Larbalestier for his stimulating interest and helpful discussions. A.G. also thanks D.K. Christen and D.O. Welch for useful comments.

APPENDIX A

Here we give necessary formulas[22] for the elastic strain tensor ϵ_{ik}. For a single dislocation, ϵ_{ik} is given by

$$\epsilon_{xx}=\frac{by[(3-2\sigma)x^2+(1-2\sigma)y^2]}{4\pi(1-\sigma)(x^2+y^2)^2}, \tag{A1}$$

$$\epsilon_{yy}=\frac{by[(1-2\sigma)y^2-(1+2\sigma)x^2]}{4\pi(1-\sigma)(x^2+y^2)^2}, \tag{A2}$$

$$\epsilon_{xy}=-\frac{bx(x^2-y^2)}{4\pi(1-\sigma)(x^2+y^2)^2}. \tag{A3}$$

For a symmetric GB, ϵ_{ik} can be obtained by replacing y by $y-nd$ and summing up over the integer n. This yields

$$\epsilon_{xx}+\epsilon_{yy}=\frac{\epsilon_b(1-2\sigma)\sin q}{\cosh p-\cos q}, \tag{A4}$$

$$\epsilon_{xx}-\epsilon_{yy}=\frac{\epsilon_b p\sin q\sinh p}{(\cosh p-\cos q)^2}, \tag{A5}$$

$$\epsilon_{xy}=-\frac{\epsilon_1(\cos q\cosh p-1)p}{2(\cosh p-\cos q)^2}, \tag{A6}$$

where $\epsilon_1=b/2(1-\sigma)d$, $p=2\pi x/d$, and $q=2\pi y/d$.

Using Eqs. (3) and (A4)–(A6), we can write the equation $T_c(x,y)=0$ for the NC core regions in the form

$$\begin{aligned}(\cosh p-\cos q)^2 h=&(\cosh p-\cos q)\sin q\\&+p_0[p\sin q\sinh p\cos 2\varphi\\&-|p|(\cosh p\cos q-1)\sin 2\varphi],\end{aligned} \tag{A7}$$

where $h=2d(1-\sigma)T_{c0}/Cb(1-2\sigma)$ and $p_0=(C_a-C_b)/(1-2\sigma)(C_a+C_b)$. Equation (A7) was used to calculate the shapes of the NC core regions in Fig. 2.

For the isotropic strain dependence of $T_c(\epsilon_{ik})$ ($p_0=0$), Eq. (A7) gives the explicit dependence $x(y)$ in the form

$$x=\frac{d}{2\pi}\cosh^{-1}\left[\cos\frac{2\pi y}{d}+\frac{1}{h}\sin\frac{2\pi y}{d}\right]. \tag{A8}$$

For the isotropic case, we can also obtain the shape of the normal NC regions $x(y)$ for the nonlinear dependence $T_c(\epsilon)$. Substituting Eqs. (A4)–(A6) into Eq. (7) and solving the quadratic equation $T_c(\epsilon)=T$ for ϵ, we get

$$x_n^{\pm}=\frac{d}{2\pi}\cosh^{-1}\left[\cos\frac{2\pi y}{d}+\frac{2\pi r_n^{\pm}}{d}\sin\frac{2\pi y}{d}\right]. \tag{A9}$$

The boundary of the dielectric NC region can be obtained by replacing $r_n^{\pm}$ by r_i^{+}. The maximum sizes x_m and y_m of the NC regions across and along GB's are given by

$$x_m^{\pm}=\frac{d}{2\pi}\ln\left[\frac{2\pi r_n^{\pm}}{d}+\sqrt{\left(\frac{2\pi r_n^{\pm}}{d}\right)^2+1}\right], \tag{A10}$$

$$y_m^{\pm}=\frac{d}{\pi}\tan^{-1}\frac{2\pi r_n^{\pm}}{d}. \tag{A11}$$

The NC regions shrink as d decreases. In the linear elasticity theory the NC regions touch only if $d\to 0$ when $y_m^{\pm}\to d/2$. However, for small d the elastic approximation becomes invalid, and the shape of the NC regions is determined by plastic and charge effects near GB's.

APPENDIX B

The equation for Φ_1,

$$\nabla^2\Phi_1-\Phi_1/l_D^2=4\pi ZeN_0\epsilon/\kappa_\infty, \tag{B1}$$

can be solved by the Fourier transformation,

$$\Phi(x,y)=\sum_G\int_{-\infty}^{\infty}\frac{dk}{2\pi}\Phi(k,G)e^{ikx+iGy}, \tag{B2}$$

where $G=2\pi n/d$ is the reciprocal lattice vector along GB's. The Fourier component $\epsilon(k,G)$ equals

$$\epsilon(k,G)=\frac{ibG(1-2\sigma)}{2d(1-\sigma)(k^2+G^2)}. \tag{B3}$$

Therefore, $\Phi_1(k,G)$ is given by

$$\Phi_1(k,G)=-\frac{2\pi iN_0Zeb(1-2\sigma)G}{d(1-\sigma)(k^2+G^2)(k^2+G^2+1/l_D^2)\kappa_\infty}. \tag{B4}$$

Substituting Eq. (B4) into Eq. (B2) and integrating over k, we arrive at Eq. (17).

Now we consider the equation for Φ_2,

$$\nabla^2\Phi_2-\Phi_2/l_D^2=4\pi ZeN_0\zeta\epsilon^2/\kappa_\infty, \tag{B5}$$

from which we obtain

$$\Phi_2(k,G)=-\frac{2e\zeta ZN_0}{(k^2+G^2+1/l_D^2)\kappa_\infty}\sum_{G'}\int\epsilon(k',G')\epsilon^*\times(k'-k,G'-G)dk'. \tag{B6}$$

Here an asterisk implies the complex conjugate, and $\epsilon(k,G)$ is given by Eq. (B3). In the coordinate representation we get

$$\Phi_2(x,y)=\frac{e\zeta ZN_0}{\pi\kappa_\infty}\sum_{G,G'}\int_{-\infty}^{\infty}dk\int_{-\infty}^{\infty}dk'\times\frac{e^{ikx+iGy}\epsilon(k',G')\epsilon(k'-k,G'-G)}{k^2+G^2+1/l_D^2}. \tag{B7}$$

The averaged in y potential $\Phi(x)=\langle\Phi_2(x,y)\rangle$ is given by the term with $G=0$ in Eq. (B7), whence

$$\Phi(x)=\frac{\zeta ZeN_0b^2(1-2\sigma)^2}{4\pi d^2(1-\sigma)^2\kappa_\infty}\sum_{G'}\int_{-\infty}^{\infty}dk\int_{-\infty}^{\infty}dk'\times\frac{e^{ikx}G'^2}{(k^2+1/l_D^2)(G'^2+k'^2)[G'^2+(k'-k)^2]}. \tag{B8}$$

Performing integrations in k and k', we arrive at Eq. (19).

APPENDIX C

We seek for the solutions of Eq. (29) with the following boundary conditions:

$$\psi(\pm\infty)=\psi_\infty,\quad \psi'(\pm\infty)=0, \tag{C1}$$

$$\psi'(+0)=-\psi'(-0)=\Gamma(\psi_0)/2. \tag{C2}$$

From Eq. (29), we obtain the integral of ''energy:''

$$\frac{1}{2}\psi'^2+U(\psi)=E, \tag{C3}$$

$$U(\psi)=\frac{\psi^2}{2}+\frac{i^2}{2\psi^2}-\frac{\psi^4}{4}, \tag{C4}$$

where $E=U(\psi_\infty)$. The boundary condition (C2) implies that the particle moving in the potential $U(\psi)$ undergoes an elastic reflection at $\psi=\psi_0$. Equation (32) for ψ_0 can be obtained for any $\Gamma(\psi)$ by substituting Eq. (C2) into Eq. (C3) at $\psi=\psi_0$.

Equation (32) has several roots which correspond to stable (s) and unstable (u) distributions $\psi(\eta,\psi_0)$ in Fig. 7. Due to the symmetry $\psi(\eta)=\psi(-\eta)$, the solution $\psi(\eta,\Gamma)$ for $\Gamma>0$ can be obtained from the solution $\psi(\eta,0)$ of Eq. (29) with $\Gamma=0$ and the same boundary conditions at $\eta\pm\infty$ by the following rule:

$$\psi(\eta,\Gamma)=\psi(|\eta|+\eta_0,0). \tag{C5}$$

Here the constant η_0 is chosen to satisfy

$$\psi_0=\psi(\eta_0,0), \tag{C6}$$

where ψ_0 is determined by Eq. (32).

The value ψ_m is determined by the condition of energy conservation, $U(\psi_\infty)=U(\psi_m)$, which enables us to factorize Eq. (C3) in the form

$$\psi'^2=(\psi_\infty^2-\psi^2)^2(\psi^2-\psi_m^2)/2\psi^2. \tag{C7}$$

Equation (C7) automatically provides the correct boundary conditions $\psi'(0)=\psi'(\pm\infty)=0$ for $\psi(\eta,0)$. Here $\eta=0$ corresponds to the value $\psi=\psi_m$ which can be found by comparing Eqs. (C3) and (C7). This gives a simple relationship between ψ_m and ψ_∞:

$$\psi_m^2=2i^2/\psi_\infty^4=2-2\psi_\infty^2. \tag{C8}$$

Equation (C7) can easily be integrated to give Eq. (30).

Now we turn to Eq. (32) which can be written in the form

$$\frac{1}{2}\left(\Gamma_1\psi_0+\Gamma_2\frac{i^2}{\psi_0^3}\right)^2=\frac{1}{\psi_0^2}(\psi_\infty^2-\psi_0^2)^2(\psi_0^2-\psi_m^2). \tag{C9}$$

Equation (C9) can be solved analytically for two limiting cases $\Gamma_2=0$ and $\Gamma_1\gg 1$. For $\Gamma_2=0$, we have

$$v-\frac{v^2}{2}+\frac{w}{v}=e, \tag{C10}$$

where $v=\psi_0^2/(1+\Gamma_1^2/4)$, $w=i^2/(1+\Gamma_1^2/4)^3$, and $e=2E/(1+\Gamma_1^2/4)^2$. The cubic equation (C10) has three roots of which only one with $dv/di<0$ corresponds to the stable $\psi(\eta)$. As seen from Fig. 7, the stable solution exists only below the critical current $i<i_c$ at which the points s and u merge. Differentiating Eq. (C9) with respect to u, we obtain

$$1-v-w/v^2=0. \tag{C11}$$

Excluding w from Eqs. (C10) and Eq. (C11), we obtain a quadratic equation for v_c, whence

$$v_c=\frac{2}{3}-\sqrt{\frac{4}{9}-\frac{2e}{3}}. \tag{C12}$$

Substituting Eq. (C12) back into Eq. (C11), we arrive after some algebra at the following equation for i_c:

$$i_c=(1-S)(1+2S)^{1/2}, \tag{C13}$$

where the function $S(i_c)$ is given by

$$S(i)=1-\frac{12\psi_\infty(4-3\psi_\infty)}{(4+\Gamma_1^2)^2}. \tag{C14}$$

In two limiting cases, Eqs. (C13) and (C14) yield the depairing current density $i_c=2/3\sqrt{3}$ at $\Gamma_1=0$ and

$$J_c=\frac{J_0}{2\Gamma_1},\quad \Gamma_1\gg 1. \tag{C15}$$

Since $J_0\propto\tau^{3/2}$ and $\Gamma_1\propto\tau^{-1/2}$, the critical current $J_c\propto\tau^2$ exhibits the temperature dependence of S-N-S Josephson contacts.[78]

Now we consider the case $\Gamma_1\gg 1$ and $\Gamma_2>0$ for which $\psi_0\propto 1/\Gamma_1\ll 1$, $\psi_\infty=1$, $\psi_m^2=2i^2$, and $i_c^2\ll 1$. Then we can retain only the term $\psi_0\Gamma_1$ and all inverse powers of ψ_0 in Eq. (C9) which thus becomes

$$\frac{1}{2}\left(\Gamma_1\psi_0+\Gamma_2\frac{i^2}{\psi_0^3}\right)^2=1-\frac{2i^2}{\psi_0^2}. \tag{C16}$$

Introducing the dimensionless parameters u, α, and q given by Eqs. (40) into Eq. (C16), we arrive at Eq. (39).

[1] D. Dimos, P. Chaudhari, and J. Mannhart, Phys. Rev. B **41**, 4038 (1990); P. Chaudhari, D. Dimos, and J. Mannhart, in *Superconductivity*, edited by J. G. Bednortz and K. A. Müller (Springer, Heidelberg, 1990).

[2] R. Gross and B. Mayer, Physica C **180**, 235 (1990).

[3] Z. G. Ivanov, P. A. Nilsson, D. Winkler, J. A. Alarco, T. Claeson, E. A. Stepantsov, and A. Ya. Tzalenchuk, Appl. Phys. Lett. **59**, 3030 (1991).

[4] M. F. Chisholm and M. F. Pennycook, Nature (London) **351**, 47 (1991).

[5] R. Gross, in *Interfaces in High-T_c Superconducting Systems*, edited by S. L. Shinde and D. A. Rudman (Springer-Verlag, New York, 1994), p. 176.

[6] T. Amerin, L. Schultz, B. Kabius, and K. Urban, Phys. Rev. B **51**, 6792 (1995).

[7] N. F. Heinig, R. D. Redwing, I-Fei Tsu, A. Gurevich, J. E. Nordman, S. E. Babcock, and D. C. Larbalestier, Appl. Phys. Lett. **69**, 577 (1996); N. F. Heinig, R. D. Redwing, J. E. Nordman, and D. C. Larbalestier (unpublished).

[8] V. B. Geshkenbein, A. I. Larkin, and A. Barone, Phys. Rev. B **36**, 235 (1987).

[9] M. Sigrist and T. M. Rice, J. Phys. Soc. Jpn. **61**, 4283 (1992); Rev. Mod. Phys. **67**, 503 (1995).

[10] H. Hilgenkamp, J. Mannhart, and B. Mayer, Phys. Rev. B **53**, 14 586 (1996).

[11] D. A. Wollman, D. J. van Harlingen, W. C. Lee, D. M. Ginsberg, and A. J. Leggett, Phys. Rev. Lett. **71**, 2134 (1993); D. J. van Harlingen, Rev. Mod. Phys. **67**, 515 (1995).

[12] C. C. Tsuei, J. R. Kirtley, C. C. Chi, L. S. Yu-Jahnes, A. Gupta, T. Shaw, J. Z. Sun, and M. B. Ketchen, Phys. Rev. Lett. **73**, 593 (1994); J. R. Kirtley, C. C. Tsui, M. Rupp, J. Z. Sun, L. S. Yu-Jahnes, A. Gupta, and M. B. Ketchen, *ibid.* **76**, 1336 (1996).

[13] D. C. Larbalestier, Science **274**, 736 (1996); IEEE Trans. Appl. Supercond. **7**, 90 (1997).

[14] L. N. Bulaevskii, J. R. Clem, L. I. Glazman, and A. P. Malozemoff, Phys. Rev. B **45**, 2545 (1992); L. N. Bulaevskii, L. L. Daemen, M. P. Maley, and J. Y. Coulter, *ibid.* **48**, 13 798 (1993).

[15] B. Hensel, G. Grasso, and R. Flükiger, Phys. Rev. B **51**, 15 456 (1995).

[16] A. Goyal, E. D. Specht, D. M. Kroeger, T. A. Mason, D. J. Dingley, G. N. Riley, Jr., and M. W. Ruppich, Appl. Phys. Lett. **66**, 2903 (1995).

[17] A. E. Pashitski, A. Gurevich, A. A. Polyanskii, D. C. Larbalestier, A. Goyal, E. D. Specht, D. M. Kroeger, J. A. De Luca, and J. E. Tkaczyk, Science **275**, 367 (1997).

[18] A. A. Polyanski, A. Gurevich, A. E. Pashitski, N. F. Heinig, R. D. Redwing, J. E. Nordman, and D. C. Larbalestier, Phys. Rev. B **53**, 8687 (1996).

[19] Y. Iijima, N. Tanabe, O. Kohno, and Y. Ikeno, Appl. Phys. Lett. **60**, 769 (1992).
[20] X. D. Wu, S. R. Foltyn, P. N. Arendt, W. R. Blumenthal, I. H. Campbell, J. D. Cotton, J. Y. Coulter, W. L. Hults, M. P. Maley, H. F. Safar, and J. L. Smith, Appl. Phys. Lett. **67**, 2397 (1995).
[21] D. P. Norton, A. Goyal, J. D. Budai, D. K. Christen, D. M. Kroeger, E. D. Specht, Q. He, B. Saffian, M. Paranthaman, C. E. Klabunde, D. F. Lee, B. C. Sales, and F. A. List, Science **274**, 755 (1996).
[22] J. B. Hirth and J. Lothe, *Theory of Dislocations* (McGraw-Hill, New York, 1968).
[23] A. P. Sutton and R. W. Balluffi, *Interfaces in Crystalline Materials* (Clarendon, Oxford, 1995).
[24] Y. Gao, K. L. Merkle, G. Bai, H. L. M. Chang, and D. J. Lam, Ultramicroscopy **37**, 326 (1991); Physica C **174**, 1 (1991).
[25] S. J. Pennycook and D. E. Jesson, Phys. Rev. Lett. **64**, 938 (1990); D. E. Jason and S. J. Pennycook, Proc. R. Soc. London, Ser. A **449**, 237 (1995).
[26] R. F. Loane, P. Xu, and J. Silcox, Ultramicroscopy **40**, 121 (1992).
[27] Y. Zhu, Z. L. Wang, and M. Suenaga, Philos. Mag. A **67**, 11 (1993).
[28] N. D. Browning, M. F. Chisholm, S. J. Pennycook, D. P. Norton, and D. H. Lowndes, Physica C **212**, 185 (1993).
[29] N. D. Browning, J. P. Buban, P. D. Nellist, D. P. Norton, M. F. Chisholm, and S. J. Pennycook, Physica C **294**, 183 (1998).
[30] A. F. Marshall and C. B. Eom, Physica C **207**, 239 (1993).
[31] S. E. Babcock and J. L. Vargas, Annu. Rev. Mater. Sci. **25**, 193 (1995); I-Fei Tsu, S. E. Babcock, and D. L. Kaiser, J. Mater. Res. **11**, 1383 (1996).
[32] E. Sarnelli, P. Chaudhari, and J. Lacey, Appl. Phys. Lett. **62**, 777 (1992).
[33] B. H. Moeckly, D. K. Lathrop, and R. A. Buhrman, Phys. Rev. B **47**, 400 (1993).
[34] E. A. Early, R. L. Steiner, A. F. Clark, and K. Char, Phys. Rev. B **50**, 9409 (1994).
[35] K. K. Likharev, Rev. Mod. Phys. **51**, 101 (1979).
[36] A. M. Campbell, Supercond. Sci. Technol. **2**, 287 (1989).
[37] J. Halbritter, Phys. Rev. B **46**, 14 861 (1992); **48**, 9735 (1993).
[38] J. Betouras and R. Joynt, Physica C **250**, 256 (1995).
[39] D. Agassi, C. S. Pande, and R. A. Masumura, Phys. Rev. B **52**, 16 237 (1995).
[40] J. A. Alarco and D. E. Olsson, Phys. Rev. B **52**, 13 625 (1995).
[41] E. Z. Meilikhov, Physica C **271**, 277 (1996).
[42] A. Gurevich and E. A. Pashitskii, Phys. Rev. B **56**, 6213 (1997).
[43] R. J. Wijngaarden and R. Griessen, in *Studies of High Temperature Superconductors*, edited by A. V. Narlikar (Nova Science, New York, 1989), Vol. 2, p. 29.
[44] J. S. Schilling and S. Klots, in *Physical Properties of High Temperature Superconductors*, edited by D.M. Ginsberg (World Scientific, Singapore, 1992), Vol. 3, p. 59.
[45] U. Welp, M. Grimsditch, S. Fleshler, W. Nessler, B. Veal, and G. W. Crabtree, J. Supercond. **7**, 159 (1994).
[46] H. Takahashi and N. Mori, in *Studies of High Temperature Superconductors*, edited by A.V. Narlikar (Nova Science, New York, 1995), Vol. 16, p. 1.
[47] C. Meingast, O. Kraut, T. Wolf, H. Wühl, A. Erb, and G. Müller-Vogt, Phys. Rev. Lett. **67**, 1634 (1991); C. Meingast, A. Junod, and E. Walker, Physica C **272**, 106 (1996).
[48] C. C. Almasan, S. H. Han, B. W. Lee, L. M. Paulius, M. B. Maple, B. W. Veal, J. W. Downey, A. P. Paulikas, Z. Fisk, and J. E. Schirber, Phys. Rev. Lett. **69**, 680 (1992).
[49] H. Ledbetter and M. Lei, J. Mater. Res. **6**, 2253 (1991).
[50] J. L. Tallon and J. R. Cooper, in *Advances in Superconductivity V*, edited by Y. Bando and H. Yamauchi (Springer-Verlag, Tokyo, 1993), p. 339; M. H. Whangbo and C. C. Torardi, Science **249**, 1143 (1990); R. P. Gupta and M. Gupta, Phys. Rev. B **51**, 11 760 (1995).
[51] D. O. Welch and R. D. Bardo, in *Advances in Superconductivity V* (Ref. 50), p. 37.
[52] G. S. Boebinger, Y. Ando, A. Passner, T. Kimura, M. Okuya, J. Shimoyama, K. Kishio, K. Tamasaku, N. Ichikawa, and S. Uchida, Phys. Rev. Lett. **77**, 5417 (1996).
[53] D. Winkler, Y. M. Zhang, P. A. Nilsson, E. A. Stepantsov, and T. Claeson, Phys. Rev. Lett. **72**, 1260 (1994).
[54] Qiang Li, Y. N. Tsay, Y. Zhu, M. Suenaga, G. D. Gu, and N. Koshizuka, Appl. Phys. Lett. **70**, 1164 (1997).
[55] B. Ya. Shapiro and I. B. Khalfin, Physica C **219**, 465 (1994); L. Burlachkov, I. B. Khalfin, and B. Ya. Shapiro, Phys. Rev. B **48**, 1156 (1993).
[56] J. Mannhart, Supercond. Sci. Technol. **9**, 49 (1996).
[57] T. Ando, A. B. Fowler, and F. Stern, Rev. Mod. Phys. **54**, 437 (1982).
[58] K. Tamasaku, Y. Nakamura, and S. Uchida, Phys. Rev. Lett. **69**, 1455 (1992); S. Tajima, G. D. Gu, S. Miyamoto, A. Odagawa, and N. Koshizuka, Phys. Rev. B **48**, 16 164 (1993).
[59] N. W. Ashcroft and N. D. Mermin, *Solid State Physics* (Saunders College, Philadelphia, 1976).
[60] In the isotropic Debye theory the Grüneisen constant is given by $\zeta=\alpha C_{11}/\nu$ (Ref. 59), where α is the thermal expansivity, C_{11} is the in-plane bulk elastic modulus, and ν is the lattice specific heat. Taking for $YBa_2Cu_3O_7$ at $T\approx T_c$, $\alpha\simeq 5\times 10^{-6}$ 1/K (Ref. 47) $\nu\simeq 1.4$ J/cm^3 (Ref. 61), and $C_{11}=230$ GPa (Ref. 49), we obtain $\alpha\approx 1$. Notice, however, that in HTS's the thermal expansivity can be essentially anisotropic even in the ab plane; for example, in $YBa_2Cu_3O_7$ the value α_b along the b axis is negative below 60 K (Ref. 47). So the simple model based on a single isotropic Grüneisen constant is used here only for a qualitative description.
[61] O. Jeandupex, A. Schilling, H. R. Ott, and A. van Otterlo, Phys. Rev. B **53**, 12 475 (1996).
[62] C. P. Poole, Jr., H. A. Farach, and R. J. Creswick, *Superconductivity* (Academic Press, San Diego, 1995).
[63] A. H. Cottrell, S. C. Hunter, and F. R. N. Nabarro, Philos. Mag. **44**, 357 (1953); S. Sugiyama, J. Phys. Soc. Jpn. **21**, 1873 (1966); R. A. Brown, Phys. Rev. **141**, 568 (1966).
[64] A. A. Abrikosov, J. C. Campuzano, and K. Gofron, Physica C **214**, 73 (1993).
[65] D. M. King, Z.-X. Shen, D. S. Dessau, D. S. Marshall, C. H. Park, W. E. Spicer, J. L. Peng, Z. Y. Li, and R. L. Greene, Phys. Rev. Lett. **73**, 3298 (1994).
[66] K. Gofron, J. C. Campuzano, A. A. Abrikosov, M. Lindroos, A. Bansil, H. Ding, D. Koelling, and B. Dabrowski, Phys. Rev. Lett. **73**, 3302 (1994).
[67] Jian Ma, C. Quitmann, R. J. Kelley, P. Almares, H. Berger, G. Margaritondo, and M. Onellion, Phys. Rev. B **51**, 3832 (1995); S. LaRosa, I. Vobornik, F. Zwick, M. Berger, M. Grioni, G. Margaritondo, R. J. Kelley, M. Onellion, and A. Chubukov, *ibid.* **56**, R525 (1997).
[68] J. R. Hurault, J. Phys. (Paris) **26**, 252 (1965).
[69] A. M. Gabovich, L. G. Il'chenko, E. A. Pashitskii, and Yu. A. Romanov, Zh. Exp. Teor. Fiz. **75**, 249 (1978) [Sov. Phys. JETP

48, 124 (1978)]; A. M. Gabovich, L. G. Il'chenko, and E. A. Pashitskii, Sov. J. Low Temp. Phys. **6**, 298 (1980).

[70] D. M. Newns, H. R. Krishnamurthy, C. C. Tsuei, P. C. Pattnaik, and C. L. Kane, Phys. Rev. Lett. **69**, 1264 (1992); D. M. Newns, C. C. Tsuei, P. C. Pattnaik, and C. L. Kane, Comments Condens. Matter Phys. **15**, 273 (1992).

[71] A. A. Abrikosov, Phys. Rev. B **56**, 446 (1997).

[72] V. V. Bulatov and E. Kaxiras, Phys. Rev. Lett. **78**, 4221 (1997).

[73] P. G. de Gennes, *Superconductivity of Metals and Alloys* (Benjamin, New York, 1966).

[74] J. J. V. Alvarez, G. C. Buscaglia, and C. A. Balserio, Phys. Rev. B **54**, 16 168 (1996).

[75] A. V. Gurevich and R. G. Mints, Rev. Mod. Phys. **58**, 951 (1987).

[76] D. G. Steel, J. D. Hettinger, F. Yuan, D. J. Miller, K. E. Gray, J. H. Kang, and J. Talvacchio, Appl. Phys. Lett. **68**, 120 (1996).

[77] Q.-H. Hu, L.-G. Johansson, V. Langer, Y. F. Chen, T. Claeson, Z. G. Ivanov, Yu. Kislinski, and E. A. Stepantsov, J. Low Temp. Phys. **105**, 1261 (1996).

[78] K. A. Delin and A. W. Kleinsasser, Supercond. Sci. Technol. **9**, 227 (1996).

[79] Yu. S. Barash, A. V. Galaktionov, and A. D. Zaikin, Phys. Rev. Lett. **75**, 1676 (1995); Phys. Rev. B **52**, 665 (1995).

[80] Y. Tanaka and S. Kashiwaya, Phys. Rev. B **56**, 892 (1997).

[81] S. Yip, J. Low Temp. Phys. **91**, 203 (1993); Phys. Rev. B **52**, 3087 (1995); M. Fogelström, S. Yip, and J. Kurkijärvi (unpublished).

[82] A. Barone and G. Patterno, *Physics and Applications of the Josephson Effect* (Wiley, New York, 1982).

[83] S. E. Babcock, X. Y. Cai, D. L. Kaiser, and D. C. Larbalestier, Nature (London) **347**, 167 (1990).

[84] C. B. Eom, A. F. Marshall, Y. Suzuki, B. Boyer, R. F. W. Pease, and T. H. Geballe, Nature (London) **353**, 544 (1991).

[85] X. Y. Cai, A. Gurevich, I-Fei Tsu, D. L. Kaiser, S. B. Babcock, and D. C. Larbalestier, Phys. Rev. B **57**, 10 951 (1998).

[86] A. Gurevich, Phys. Rev. B **46**, R3187 (1992); **48**, 12 857 (1993); A. Gurevich and L. D. Cooley, *ibid.* **50**, 13 563 (1994).